

This is a repository copy of *Interferences in photolytic NO₂ measurements: explanation for an apparent missing oxidant?*.

White Rose Research Online URL for this paper:

<https://eprints.whiterose.ac.uk/99217/>

Version: Accepted Version

Article:

Reed, C., Evans, M. J. orcid.org/0000-0003-4775-032X, Di Carlo, P. et al. (2 more authors) (2016) Interferences in photolytic NO₂ measurements: explanation for an apparent missing oxidant? *Atmospheric Chemistry and Physics*. pp. 4707-4724. ISSN 1680-7324

<https://doi.org/10.5194/acp-16-4707-2016>

Reuse

This article is distributed under the terms of the Creative Commons Attribution (CC BY) licence. This licence allows you to distribute, remix, tweak, and build upon the work, even commercially, as long as you credit the authors for the original work. More information and the full terms of the licence here:

<https://creativecommons.org/licenses/>

Takedown

If you consider content in White Rose Research Online to be in breach of UK law, please notify us by emailing eprints@whiterose.ac.uk including the URL of the record and the reason for the withdrawal request.

Interferences in photolytic NO₂ measurements: explanation for an apparent missing oxidant?

C. Reed¹, M. J. Evans^{1,2}, P. Di Carlo^{3,4}, J. D. Lee^{1,2}, and L. J. Carpenter¹

¹Wolfson Atmospheric Chemistry Laboratories, Department of Chemistry, University of York, Heslington, York, YO10 5DD, UK

²National Centre for Atmospheric Science (NCAS), University of York, Heslington, York, YO10 5DD, UK

³Centre of Excellence CEMTEPs, Universita' degli studi di L'Aquila, Via Vetoio, 67010 Coppito, L'Aquila, Italy

⁴Dipartimento di Scienze Fisiche e Chimiche, Universita' degli studi di L'Aquila, Via Vetoio, 67010 Coppito, L'Aquila, Italy

Correspondence to: J. D. Lee (james.lee@york.ac.uk)

Abstract

Measurement of NO_2 at low concentrations (10s ppt) is non-trivial. A variety of techniques exist, with the conversion of NO_2 into NO followed by chemiluminescent detection of NO being prevalent. Historically this conversion has used a catalytic approach (molybdenum); however this has been plagued with interferences. More recently, photolytic conversion based on UV-LED irradiation of a reaction cell has been used. Although this appears to be robust there have been a range of observations in low NO_x environments which have measured higher NO_2 concentrations than might be expected from steady state analysis of simultaneously measured NO , O_3 , $j\text{NO}_2$ etc. A range of explanations exist in the literature most of which focus on an unknown and unmeasured “compound X ” that is able to convert NO to NO_2 selectively. Here we explore in the laboratory the interference on the photolytic NO_2 measurements from the thermal decomposition of peroxyacetyl nitrate (PAN) within the photolysis cell. We find that approximately 5% of the PAN decomposes within the instrument providing a potentially significant interference. We parameterize the decomposition in terms of the temperature of the light source, the ambient temperature and a mixing timescale ($\sim 0.4\text{ s}$ for our instrument) and expand the parametric analysis to other atmospheric compounds that decompose readily to NO_2 (HO_2NO_2 , N_2O_5 , $\text{CH}_3\text{O}_2\text{NO}_2$, IONO_2 , BrONO_2 , Higher PANs). We apply these parameters to the output of a global atmospheric model (GEOS-Chem) to investigate the global impact of this interference on (1) the NO_2 measurements and (2) the NO_2 : NO ratio i.e. the Leighton relationship. We find that there are significant interferences in cold regions with low NO_x concentrations such as the Antarctic, the remote Southern Hemisphere and the upper troposphere. Although this interference is likely instrument specific, it appears that the thermal decomposition to NO_2 within the instrument’s photolysis cell may give an explanation for the anomalously high NO_2 that has been reported in remote regions. Better instrument characterization, coupled to instrumental designs which reduce the heating within the cell seem likely to minimize the interference in the future, thus simplifying interpretation of data from remote locations.

1 Introduction

Accurate quantification of atmospheric nitrogen oxides (NO_x which is predominantly $\text{NO} + \text{NO}_2$ but includes small contributions from NO_3 , N_2O_5 , HONO , HO_2NO_2 etc.) concentrations is crucial for many aspects of tropospheric chemistry. NO_x plays a central role in the chemistry of the troposphere, mainly through its impact on ozone (O_3) and hydroxyl (OH) radical concentrations. O_3 is a greenhouse gas (Wang et al., 1995), adversely impacts human health (Mauzerall et al., 2005; Skalska et al., 2010) and leads to ecosystem damage (Ainsworth et al., 2012; Ashmore, 2005; Hollaway et al., 2012). It is produced through the reaction of peroxy radicals (HO_2 and RO_2) with NO (Dalsøren and Isaksen, 2006; Lelieveld et al., 2004). The OH radical is the primary oxidizing agent in the atmosphere (Crutzen, 1979; Levy II, 1972) as it controls the concentration of other key atmospheric constituents such as methane (CH_4), carbon monoxide (CO) and volatile organic compounds (VOCs). It is both produced through the reaction of NO with HO_2 and is lost by its reaction with NO_2 . NO_2 itself also poses a public health risk (Stieb et al., 2002). Thus understanding the sources, sinks and distribution of NO_x is of central importance to understanding the composition of the troposphere.

During the daytime there is fast cycling between NO and NO_2 , due to the rapid photolysis of NO_2 and the reaction NO and O_3 to form NO_2 (Kley et al., 1981).



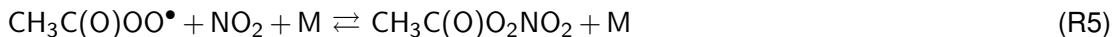
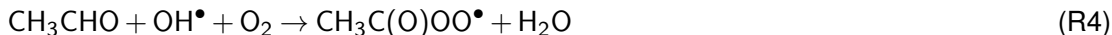
Placing NO_2 into steady state and assuming that these three reactions are the only chemistry occurring leads to the Leighton relationship, ϕ (Leighton, 1961), in Eq. (1).

$$1 = \frac{k_1 [\text{NO}] [\text{O}_3]}{j_{\text{NO}_2} [\text{NO}_2]} = \phi \quad (1)$$

The quantities in the relationship are readily measured and deviations from unity have been interpreted to signify missing (i.e. non ozone) oxidants of NO . These perturbations

have been used to infer the existence of oxidants such as peroxy radicals, halogen oxides, and the nitrate radical in the atmosphere which have subsequently been confirmed by direct measurement (Brown et al., 2005, Mannschreck et al., 2004, Trebs et al., 2012, Volz-Thomas et al., 2003).

The concentration of NO_x varies from > 100 ppb (parts per billion) next to roads (Carslaw, 2005; Pandey et al., 2008) to low ppt (parts per trillion) in the remote atmosphere (Lee et al., 2009). Direct transport of NO_x from polluted to remote regions is not efficient, because NO_x is removed from the atmosphere on a timescale of around a day by the reaction of NO_2 with OH and the hydrolysis of N_2O_5 on aerosol surfaces (Brown et al., 2004; Dentener and Crutzen, 1993; Riemer et al., 2003). Instead, reservoir species such as peroxy-acetyl nitrate are made in polluted regions (where concentrations in both NO_x and peroxy-acetyl precursors such as acetaldehyde are elevated) and are subsequently transported to remote regions where they thermally breakdown to release NO_x (Fisher et al., 2014; Moxim et al., 1996; Roberts et al., 2007).



The equilibrium between peroxy-acetyl radicals, NO_2 and PAN (Reactions R4 and R5) is highly temperature sensitive. Thus the PAN lifetime changes from 30 min at 25°C (Bridier et al., 1991) to 5.36 years at -26°C (Kleindienst, 1994).

Measurements of NO_x species in the remote atmosphere have been made over the last 40 years. Multiple in-situ techniques are available such as LIF - Laser Induced Fluorescence (Matsumoto and Kajii, 2003), CRDS - Cavity Ring Down Spectroscopy (Osthoff et al., 2006), and QCL - Quantum Cascade Laser (Tuzson et al., 2013). However, probably the most extensively used approach has been based on the chemiluminescent reaction between NO and O_3 . This exploits the reaction between NO and O_3 (Reaction R6) which generates an electronically excited NO_2^* (2B_1) molecule which decays to its ground state through the

release of a photon (Reaction R7) (Clough and Thrush, 1967; Clyne et al., 1964).



This forms the basis of the chemiluminescence analysis of NO (Drummond et al., 1985; Fontijn et al., 1970; Kelly et al., 1980; Peterson and Honrath, 1999). The number of photons emitted by the decay of excited NO_2^* to NO_2 is proportional to the NO present before reaction with O_3 (Drummond et al., 1985). The photons emitted are detected by a cooled photomultiplier tube (PMT) with the sample under low pressure (to maximize the fluorescence lifetime of the NO_2^*), to yield a signal which is linearly proportional to the number density of NO in the sample gas (Fontijn et al., 1970). Quenching of the NO_2 excited state occurs due to a range of atmospheric compounds (N_2 , Ar, CO, CO_2 , CH_4 , O_2 , He, H_2 , and H_2O) (Clough and Thrush, 1967; Drummond et al., 1985; Zabielski et al., 1984). Quenching is minimised by operating at high vacuum to reduce collision probability, however quenching still occurs thus it is necessary to calibrate the detectors response (sensitivity) to a known concentration of NO regularly. Changing ambient humidity in the sample has a great effect on drift in sensitivity and necessitates correcting for, sample drying, or sample humidifying to mitigate.

With NO chemiluminescence analysers it is also possible to analyse NO_2 if it is first converted to NO, either catalytically (typically heated molybdenum) as in Reaction (R8) (Villena et al., 2012), or by converting NO_2 into NO photolytically (Ryerson et al., 2000), exploiting Reaction (R1).



To measure NO and NO_2 , the sample flows through the NO_2 to NO converter (of either type) to the reaction chamber where the $\text{NO} + \text{O}_3$ reaction occurs and the decay of NO_2^* to NO_2 allows the concentration of $\text{NO} + \text{NO}_2$ in the air to be measured. Then, the sample flow is switched to bypass the NO_2 to NO converter. Now, only NO present in the sample is detected in the chemiluminescence reaction. The NO signal is then subtracted from the

NO + NO₂ (NO_x) signal giving the NO₂ signal. Both techniques for converting NO₂ to NO can be subject to interference. Catalytic conversion has been well documented to have positive responses to NO_y species such as nitrous and nitric acid as well as organic nitrates (Dunlea et al., 2007; Grosjean and Harrison., 1985; Winer et al., 1974). Photolytic conversion has been previously demonstrated to be affected by a negative interference from the photolysis products of VOCs reacting with NO within the photolysis cell (Villena et al., 2012) and the possibility for positive interference from thermal decomposition of NO_y recognised (McClenny et al., 2002).

Measurements of NO and NO₂ have been made in a range of low NO_x locations using the chemiluminescence technique (Huntrieser et al., 2007; Lee et al., 2009; Peterson and Honrath, 1999; Zhang et al., 2008). Measurement of NO_x by the NO chemiluminescent technique in these locations can be challenging (Yang et al., 2004), often operating close to the limit of detection (LOD). Corrections may be necessary for oxidation of NO to NO₂ in the inlet by O₃ and more problematic, by peroxy radicals produced by e.g. PAN decomposition within the inlet. This oxidation acts to perturb the observed Leighton relationship in two ways; by release of NO₂ and by oxidation of NO. Where NO and NO₂ are measured by 1 channel by switching the UV elements on and off periodically there may be a greater discrepancy in the Leighton ratio as NO is oxidised to NO₂ by peroxy radicals produced from the thermal decomposition of PAN within the still-warm, but not illuminated, NO₂ converter. However, we have shown there to be less PAN decomposition in a switched system owing to generally lower LED temperatures, thus the effect on the Leighton ratio is not immediately obvious. Small corrections for NO offset are typically made by taking a stable nighttime value (Lee et al., 2009), whilst NO₂ offset must often be taken when sampling a source of zero air (which may be used for NO if a stable nighttime value is not obtainable). Correction for changing NO₂ photolytic conversion efficiency due to O₃ in the photolysis cell (see Sect. 2.2, Eq. 2) might also be appropriate when O₃ varies greatly or calibration in ambient air is not possible i.e. instead in zero air which necessarily contains no O₃.

Yang et al., (2004) identified a statistical source of error when determining NO and NO₂ by chemiluminescence. Yang et al. demonstrate that uncertainties in averaging signals which

fall below ~ 10 times the 1σ limit of detection result large errors in $\text{NO}_2:\text{NO}$ ratio, with extreme bias exhibited when signals fall below a signal to noise ratio ~ 5 . The outcome being that using weighted geometric mean, rather than unweighted or arithmetic mean for averaging PMT counts to determine NO and NO_x to then calculate NO_2 results in the least bias from measurement uncertainty. This error is in addition to any artifact signal biasing either NO or NO_2 , uncertainties in NO_2 conversion efficiency etc.

Some measurements made in remote (low NO_x) locations, such as Antarctica and in the open ocean have at times identified an unexplained imbalance in the Leighton relationship (Bauguitte et al., 2012; Frey et al., 2013, 2015; Hosaynali Beygi et al., 2011). Measured NO_2 concentrations are higher than would be expected from the observed NO, O_3 , JNO_2 along with reasonable concentrations of other oxidants (peroxy radicals, halogen oxides). Various explanations have been posited in order to overcome the apparent oxidation gap, typically relying on a mystery unmeasured oxidant, or pushing known chemistry into theoretical realms by theorizing high turnover of short-lived species which may only have been measured in trace quantities (Cantrell et al., 2003; Frey et al., 2013, 2015; Hosaynali Beygi et al., 2011). An alternative explanation would be an unknown interference on the NO_2 measurement increasing its apparent concentration, if this interference has a similar diurnal concentration profile.

Here we explore the potential of PAN (as a probe for other NO_y species) to interfere with chemiluminescence NO_2 measurements. In Sect. 2 we provide details of the experimental studies undertaken. In Sect. 3 we describe the results of experiments introducing differing concentrations of PAN into NO_2 converter/chemiluminescence systems. In Sect. 4 we analyse the potential for errors with different NO_x systems to investigate the interference on the measurement of NO_2 from PAN. In Sect. 5 we evaluate the impact of this interference on NO_2 measurements and on the Leighton relationship through the use of a global model and provide conclusions in Sect. 6.

2 Experimental details

In Sect. 2.1 we describe the two chemiluminescence instruments used for the analysis. The NO_2 converters are described in Sect. 2.2. In Sect. 2.3 the LIF instrument used to provide a reference analysis is described. We describe our protocol for production of PAN by acetone photolysis in Sect. 2.4. We provide details of the zero air generation in Sect. 2.5. Then in Sect. 2.6 we describe the experimental methodology of PAN interference tests and Sect. 2.7 describes residency time tests.

2.1 Instrumentation

Chemiluminescent measurements were performed using dual channel Air Quality Design Inc. (Golden, Colorado, USA) instruments equipped with UV-LED based photolytic NO_2 converters – commonly referred to as Blue Light Converters (BLCs). Two similar instruments were employed; the “laboratory” NO_x analyser (Sect. 2.1.1) – on which the majority of the experiments were performed and the “aircraft” NO_x analyser (Sect. 2.1.2) on which only temperature controlled BLC experiments were performed.

Both instruments feature independent mass flow controlled sample flows on each channel (NO and NO_x). The wetted surfaces of the instrument are constructed of 1/4 inch PFA tubing, with the exception of 316 stainless steel unions/MFC internals.

Both instruments are calibrated for NO by internal, automatic standard addition. Calibration for NO_2 converter efficiency is by internal automatic gas phase titration of NO with O_3 to form NO_2 with the NO signal measured with the BLC lamps active and inactive as described by Lee et al., (2009). Artifacts in both NO and NO_2 are measured whilst sampling zero air.

2.1.1 Laboratory NO_x analyser

The laboratory NO_x analyser from Air Quality Design, Inc. (AQD) is a custom dual channel instrument designed for fast response and very low limit of detection (LOD) of 2.5 pptv averaged over 1 minute. The dual channel design means that there are effectively two separate

NO chemiluminescence instruments working in parallel. Both channels have identical flow paths and share identical duplicate equipment; ozonizers, MFCs, PMTs etc. Both channels share the same vacuum pump – an Edwards XDS 35i. One channel is equipped with a BLC immediately in front of the MFC flow control/low pressure side of the system. It is possible to analyse NO with one channel, and NO_x with the other to provide a constant, fast measurement (1 Hz) of NO and NO_2 . Alternatively, a single channel can be used with the BLC in a switching mode so that it is active for only 40 % of the duty cycle to provide NO and NO_2 measurement – the other 60 % of the duty cycle is devoted to NO (40 %) and to measuring zero (20 %). In this case the second channel might be used for NO_y by connection of a catalytic converter to the inlet as is the set-up at the Cape Verde Atmospheric Observatory GAW station (Lee et al., 2009). In these experiments both modes were used in order to replicate different instrument designs; a switching mode with 40 % duty cycle of the NO_2 converter and a total sample flow of 1 standard L min^{-1} , and a parallel mode with 100 % duty cycle of the NO_2 converter with a total sample flow of 2 standard L min^{-1} . Photochemical zero is determined for 30 seconds every 5 minutes. A photochemical zero is acquired by increasing the $\text{NO} + \text{O}_3$ reaction time by diverting the sample flow to a pre-reactor where greater than 99 % of NO is reacted. The pre-reactor is a Teflon volume immediately prior to the detection cell though which usually only O_3 flows, but which during zero both the sample gas and O_3 flow. In this way, photon counts arising from slower (~ 2 orders of magnitude) alkene + O_3 reactions are accounted for and subtracted from the NO signal.

The nominal sensitivity of the instrument is 3.5 and 4.0 $\text{counts s}^{-1} \text{ ppt}^{-1}$ ($\pm 5\%$) on channel 1 (NO) and channel 2 (NO and NO_x) respectively. The $\pm 5\%$ uncertainty arises from the error in the NO standard concentration, the error of the sample and standard mass flow controllers, and the reproducibility of the sensitivity determination. Sensitivity drift was mitigated by performing all experiments under an overflow of stable zero air, thus no changes in e.g. humidity, which affects chemiluminescent quenching, occurred. The 1 min LOD (2σ) is ~ 2.5 pptv.

2.1.2 Aircraft NO_x analyser

The aircraft NO_x analyser, also from AQD, operates similarly to the lab NO_x analyser with some alterations to make it suited to aircraft operation. These changes do not affect its use on the ground. It can therefore be considered analogous to the lab NO_x analyser with the exception of the BLC. This is of a non-standard design that uses six more powerful UV-diodes which require active Peltier/forced air-cooling in order to maintain an operating temperature close to ambient. The special requirements for this NO₂ converter are primarily because of the high sample flow rates needed to measure NO_x fluxes on an airborne platform at reduced pressure. However, in this study the sample flow rate was a constant 1 standard L min⁻¹ per channel at ambient temperature and pressure.

The nominal sensitivity of the instrument is 8.3 and 11.6 counts s⁻¹ ppt⁻¹ (±5%) on channel 1 (NO) and channel 2 (NO_x) respectively. The 1 min LOD (2 σ) is ~ 1.0 pptv.

2.2 NO₂ converters

Photolytic converters for the two chemiluminescent systems were supplied by Air Quality Design and manufactured according to their proprietary standards (Buhr, 2004, 2007). Systems have also been developed subsequently (Pollack et al., 2011; Sadanaga et al., 2010) with variations implementation, though similar operation and results. Experiments with either NO₂ converter were carried out at ambient temperature and pressure; 20 °C, 1 atm.

Photolytic converters employ Reaction (R1) to convert NO₂ to NO over a narrow wavelength band, thus providing a more selective NO₂ measurement to that provided by molybdenum catalysts (Ridley et al., 1988; Ryerson et al., 2000). The conversion efficiency is determined by Eq. (2) where t is the residence time within the photolysis cell. Here $k[\text{Ox}]$ is the concentration and rate constant of any oxidant that reacts with NO to form NO₂ (Ryerson et al., 2000).

$$\text{CE} = \left[\frac{jt}{jt + k[\text{Ox}]t} \right] \left[1 - \exp(-jt - k[\text{Ox}]t) \right] \quad (2)$$

The rate constant of photolysis of NO_2 (j), and so, the rate of production of additional NO beyond that in the original sample is given in Eq. (3).

$$j(T) = \int_{\lambda \text{ min}}^{\lambda \text{ max}} F(\lambda) \sigma(\lambda, T) \phi(\lambda, T) d\lambda \quad (3)$$

In Eq. (3) j is the rate constant (s^{-1}), F is the spectral photon flux ($\text{photons cm}^{-2} \text{s}^{-1} \text{nm}^{-1}$), σ is the absorption cross section of NO_2 (cm^2), ϕ is the quantum yield (dimensionless) of NO_2 photo-dissociation, and T is the temperature (Sander et al., 2011). The j value of the converter is practically determined by the irradiance photolysis power of the UV emitting elements and how efficiently the power is used.

2.2.1 Standard BLC

Standard BLCs consist of two ends housing the UV-LEDs (1 W, 395 nm, UV Hex, Norlux Corp) within a heat sink to which is attached a cooling fan. The ends are bolted to a central section with rubber gaskets forming an air-tight seal. Within the centre section a propriety Teflon-like material block is housed which serves as a highly UV reflective (> 0.95) cavity through which the sample gas flows (Buhr, 2007). On two of the opposing sides of the centre section are 1/4 inch Swagelok fittings acting as an inlet and outlet for the sample gas.

The volume of this illuminated sample chamber is 16 mL which, with a standard flow rate of 1 standard L min^{-1} , gives a sample residence time of 0.96 s. Additional lamp end units were also supplied by AQD.

The conversion efficiency of the standard BLC with a sample flow of 1 standard L min^{-1} was between 22 and 42% ($j = 0.2 \dots 0.6 \text{s}^{-1}$) depending on the combination of lamp units used whilst the external temperature of the converter was typically 34 to 45 °C. All experiments were carried out at with sample gas at ambient temperature and pressure; 20 °C, 1 atm.

2.2.2 High power BLC

The high power BLC of the aircraft instrument is designed to operate at a higher flow rate ($1.5 \text{ standard L min}^{-1}$), lower pressure ($\sim 300 \text{ Torr}$) and therefore lower residence time, to that of the standard BLC to allow fast time resolution measurements from an aircraft. For this reason a greater number (six) of more powerful UV-LEDs [2W, 395 nm, Nichia Corp] are used in order that the conversion efficiency be acceptable under these conditions. The lamps are placed evenly along two sides of a cylindrical cavity of the same highly UV reflective Teflon with inlets at opposing ends. The high power BLC lamps are actively (Peltier) cooled to 47°C , and without Peltier cooling reached 77°C . It was therefore possible to control the internal temperature of the BLC by varying the power supplied to the Peltier elements via the temperature controller.

The volume of this illuminated sample chamber is 10 mL which, with a standard flow rate of $1 \text{ standard L min}^{-1}$, gives a sample residence time of 0.60 s resulting in a conversion efficiency of 93 % ($j = 6.5 \text{ s}^{-1}$).

2.3 TD-LIF analyser

Laser induced fluorescence (LIF) provides a direct NO_2 measurement, as opposed to chemiluminescence with conversion. A direct method of NO_2 determination to compare with the BLC NO_2 converters is desirable in order to properly know the source of any “artifact” NO_2 signal.

The Thermal Dissociation Laser Induced Fluorescence (TD-LIF) system is a custom instrument developed for aircraft and ground-based observations of NO_2 , $\sum\text{PNs}$, $\sum\text{ANs}$, and HNO_3 . A detailed description of the TD-LIF instrument can be found in Di Carlo et al. (2013), with a short description given here. It uses LIF to detect NO_2 concentrations directly (Dari-Salisburgo et al., 2009; Matsumoto and Kajii, 2003; Matsumoto et al., 2001; Thornton et al., 2000) and, coupled with a thermal dissociation inlet system, allows measurement of peroxy nitrates ($\sum\text{PNs}$), alkyl nitrates ($\sum\text{ANs}$), and HNO_3 after conversion into NO_2 (Day et al., 2002). The TD-LIF comprises four main parts: the laser source, the detection cells system,

the inlet system and the pumps. The laser source is a Nd:YAG pulse doubled laser (Spectra-Physics, model Navigator I) that emits light at 532 nm with a power of 3.8 W, a repetition rate of 15 kHz and 20 ns pulse-width. The detection cells system comprises four identical cells, one for each compound class, to allow simultaneous measurements. Each cell is formed by a cube and two arms where the laser beam passes through the sample air flow in the centre of the cell. Perpendicular to both (laser beam and air flow) there is the detector that is a gated photomultiplier with lens and long pass filters to optimize the fluorescence detection, minimizing the non-fluorescence light that reaches the detector (Di Carlo et al., 2013; Dari-Salisburgo et al., 2009). The pump system includes a roots blower coupled to a rotary vane pump to maintain a flow of 6 L min^{-1} . The common inlet system is split in four channels: one at ambient temperature to measure NO_2 , and the last three heated at 200, 400 and 550°C , to thermally dissociate ΣPNs , ΣANs , and HNO_3 respectively into NO_2 (Di Carlo et al., 2013). To minimize quenching due to atmospheric molecules, and therefore increase the sensitivity of the TD-LIF, each cell is kept at low pressure (3–4 Torr). This increases the fluorescence lifetime and facilitates the time-gating of the photomultiplier to further reduce the background (Dari-Salisburgo et al., 2009). The TD-LIF is routinely checked for background by an over-flow of zero air in the detection cells; and calibrated by standard addition of known amount of NO_2 from a cylinder (NIST traceable) diluted in zero air – the flow of both zero air and NO_2 being MFC controlled. The time resolution of the measurements is 10 Hz and the detection limits are: 9.8, 18.4, 28.1, and 49.7 pptv (1 s, $S/N = 2$) for NO_2 , ΣPNs , ΣANs , and HNO_3 cells, respectively (Di Carlo et al., 2013).

2.4 PAN preparation

In order to test the sensitivity of the instrument to peroxy-acetyl nitrate (PAN) interferences it was prepared by the photolysis in air of acetone and NO as described by (Meyrahn et al., 1987) and later by (Warneck and Zerbach, 1992; Flocke et al., 2005). Reactions (R9)–(R13) show the reaction sequence by which PAN is formed by acetone photolysis (Singh et al.,

1995)



Here, NO_2 reacts stoichiometrically with the peroxy acetyl radical to form PAN. In practice, an excess of acetone is used to ensure that NO reacts completely. A dedicated “PAN generator”, as used by Whalley et al. (2004), was employed to produce a consistent source of > 95 % pure PAN (Flocke et al., 2005; Mills et al, 2007). The generator consists of: flow control elements for the NO standard gas, the acetone flow, and the zero air diluent flow; a thermo-stated (30°C) acetone permeation oven consisting of a reservoir of HPLC grade acetone (ACS grade, Acros) with a silicone permeation tube placed in the headspace through which zero air flows; and a Pyrex glass photolysis cell illuminated by UV light centred at 285 nm (Pen-Ray mercury lamp, UVP). The Pyrex functions to filter wavelengths below 290 nm within the photolysis cell thus minimizing PAN photolysis (Mills et al., 2007).

A minor product also found in the photolysis of acetone is methyl nitrate, MeONO_2 , which is typically approximately 1 % of the total yield (Mills et al., 2007). The proposed origin of the methyl nitrate (Williams et al., 2014) is shown in Reaction (R14) and formaldehyde which is presumed to make up the balance is shown in (R15) (Singh et al., 1995; Warneck and Zerbach, 1992).



Methyl nitrate is also found in the atmosphere through oceanic emission (Moore and Blough, 2002) and as a product of the thermal decomposition of PAN (Fischer and Nwankwoala, 1995; Roumelis and Glavas, 1992; Warneck and Zerbach, 1992).

All flow rates within the PAN generator were calibrated using a Gilian Gilibrator-2 Air Flow Calibrator (Sensidyne). The PAN generator is capable of continuously producing 0.1–20.0 ppbv PAN. Linearity and mixing ratio of the PAN output was confirmed by PAN-GC equipped with an ECD detector as described by Whalley et al. (2004), and also by complete reduction back to NO using a heated (325 °C) molybdenum catalyst (Thermo Environmental). The Laser Induced Fluorescence instrument, described in Sect. 2.2.3, was used to quantify NO₂ produced directly in the PAN generator, which other authors (Flocke et al., 2005) have found to be the main impurity, with the results presented in Sect. 2.6 showing that $\leq 1\%$ NO₂ is emitted directly.

2.5 Zero air

Zero air was generated from dried ($-40 T_d$) compressed air by subsequent filtering through a cartridge of molecular sieve (13 \times , Sigma Aldrich) to ensure a consistent humidity throughout all experiments and was regenerated by heating to 250 °C for 24 h when necessary. A second filter cartridge placed after the molecular sieve was packed with Sofnofil (Molecular Products) and activated charcoal (Sigma Aldrich) in order to remove ozone, NO_x, and volatile organic compounds (VOC) which may be present in the compressed air. Zero air generated from the compressed air and filter cartridges system and zero air from an Eco Physics AG PAG 003 pure air generator (the industry standard) were both sampled by the NO chemiluminescence analyser. No difference in the counts of the NO analyser was observed between the two sources of zero air, both showing below the LOD levels of NO (< 2.5 pptv). Thus the NO content of both sources of zero air was considered to be insignificant and comparably low.

The NO₂ content of any zero air used is critical (more so than NO) in this study. In order to determine the NO₂ content of the zero air sources a direct measurement of NO₂ was required in order to avoid biasing the experimental procedure. The LIF instrument described in Sect. 2.2.3 was used to compare the zero air sources (Table 1).

Zero air from both PAG 003 and filter stack was sampled by the NO₂ LIF analyser. Additionally, high grade bottled zero air (BTCA 178, BOC Specialty Gasses) was analyzed

for NO_2 . Table 1 shows the photomultiplier counts s^{-1} whilst sampling 1.5 standard L min^{-1} of zero air. The dark counts of the PMT in the absence of laser light are typically less than 3 counts s^{-1} . The counts recorded are therefore the sum of any NO_2 fluorescence and scattered laser light. It is clear that the Sofnofil/Carbon filter system has an advantage over both the PAG 003 and BTCA 178 zero air sources in that a lower signal for NO_2 fluorescence was observed. Typical sensitivity of the LIF NO_2 channel was ~ 180 counts s^{-1} ppb^{-1} , thus a 4 – 4.5 counts s^{-1} improvement in zero background equates to 22 – 25 ppt improvement in accuracy. Consequently, all dilution, zeroing, and PAN generation utilized the Sofnofil/Carbon filter system.

2.6 Experimental procedure

The NO_x analysers were first calibrated for sensitivity/converter efficiency whilst sampling zero air by overflowing the inlet from the internal source prior to the experiment for at least 2 h. This is because the PAN from the generator is in zero air which has a very low dew point (-40 T_d) and the sensitivity of the NO_x analyser is reduced by high humidity in ambient sample gas. This means that switching the NO_x analyser from sampling ambient (humid) air to zero air causes the sensitivity to rise slowly and the humidity inside of the reaction cell to decrease. After establishing an NO flow (4.78 ppm NO in N_2 , BOC specialty gases) of 0.5 mL min^{-1} into the PAN generator, the acetone flow was then adjusted to ~ 10 mL min^{-1} and the diluent flow of zero air adjusted to achieve the desired output mixing ratio. The internal zero air of the NO_x analyser was then shut off so that the NO_x analyser was sampling zero air from the PAN generator. Note that the total flow from the PAN generator always exceeded the sample requirements of the NO_x analyser with excess flow vented to the atmosphere. The system was then allowed to stabilize until a consistent NO value was recorded on the NO_x analyser. Next, the acetone photolysis lamp of the PAN generator was switched on so that acetone was photolysed in the presence of NO to form PAN. Complete NO conversion to PAN was indicated by the fact that in all cases the NO signal measured by the NO_x analyser fell to ~ 0 ppbv after the acetone/NO mixture was illuminated by the photolysis lamp; $> 99.5\%$ conversion was reported by Mills et al.,

(2007) with the same system. The diluent flow from the PAN generator was then varied to achieve PAN mixing ratios of between 0.2 to 1.3 ppbv. The corresponding NO₂ signal was recorded once stable. This procedure was repeated for various combinations of BLC lamps/assemblies and analyser operation modes.

In order to investigate any interference from unreacted acetone, the NO_x analyser was allowed to sample the output of the PAN generator with the photolysis lamp off i.e. a flow of acetone and NO gas. No additional NO₂ signal relative to zero air was observed during these experiments at any mixing ratio of NO.

To investigate any interference from unreacted peroxy radicals left over from photolysis of excess acetone, produced in (R6), the NO_x analyser was allowed to sample acetone that had been photolysed within the PAN generator in the absence of NO. NO was then added downstream of the photolysis cell at the NO_x analyser inlet. In this way, any peroxy radicals exiting the PAN generator will cause a loss of NO and a production of NO₂ which can be quantified. No loss of NO or production of NO₂ was observed indicating that peroxy radicals from acetone photolysis within the PAN generator do not have a long enough lifetime (self reaction or surface loss) before entering the BLC, to cause an interference or 'PERCA' (Clemmitshaw et al., 1997) like chemistry within the BLC.

It should be noted that sampling acetone does cause a small increase in the chemiluminescent zero count (a few hundred counts on a signal of ~ 4000) of the NO_x analyser as acetone does react with ozone; this chemiluminescence interference is known (Dunlea et al., 2007) and is accounted for in the measurements by the photochemical zero taken every 5 minutes described in Sect. 2.1.1.

To test whether the PAN generator produced any NO₂ directly (i.e. rather than as a consequence of decomposition of PAN to NO₂ within the BLC), a direct measurement of NO₂ was employed using the TD-LIF described in Sect. 2.2.3. The measured signal relative to pure zero air was measured in the LIF NO₂ channel when sampling various mixing ratios of PAN from the generator as shown in Fig. 1. It is evident that the NO₂ signal observed while sampling PAN from the generator lies within the noise of the zero signal measurement. In this case each point represents a 10 min average as does the zero measurement. With

an averaging time of 10 min the theoretical limit of detection is estimated to be less than 0.1 pptv – taking a 10 Hz LOD of 9.8 pptv, and averaging 6000 points (i.e. 10 min) the precision improves by a factor of approximately $1/\sqrt{n}$ where n is the number of points averaged (Lee et al., 2009). It is therefore conservatively estimated that < 10 ppt NO_2 at 1000 ppt PAN ($< 1\%$) is produced by the PAN generator. This is less than previously estimated (Mills et al., 2007), albeit at higher PAN mixing ratios and lower residence times within the acetone photolysis cell with the same generator.

It was therefore determined that only PAN could be an interfering species in the BLC from the PAN generator. The small percentage of methyl nitrate which may be produced is discounted due to it being less thermally labile than PAN itself. Additionally, the percentage interference observed is significantly greater than any expected or reported methyl nitrate yield from PAN synthesis by acetone photolysis i.e. 1% (Mills et al., 2007). In the following discussion we address the possibility of photolytic and thermal dissociation of PAN or methyl nitrate to NO_2 and subsequently NO within the photolytic convertor.

2.7 Residence time

The residence time of PAN in the 2.7 m PFA inlet linking the PAN generator to the NO_x analysers (shown in Table 2) was varied by varying the flow rate. This was achieved by altering the sample flows through the each of the NO_x analyser channels (which share a common inlet). Residence times were 2.10 and 1.05 s^{-1} for 1 and 2 channel operation respectively.

3 Impact of PAN on NO_2 measurements

In this section we describe experiments investigating the impact of PAN on the two NO_2 instruments measurements. In Sect. 3.1 and 3.2 we explore the interference in the laboratory instrument with a range of BLC convertors, eliminating any possibility for inlet effects in Sect. 3.3, and in Sect. 3.4 we explore the interference in the aircraft instrument which has an active cooling of the convertor. In Sect. 3.5 we investigate whether photolytic de-

composition of PAN could lead to the interferences and in Sect. 3.6 we investigate whether thermal decomposition could be the source.

3.1 Standard BLC and laboratory NO_x analyser in constant mode

PAN was introduced to the laboratory NO_x analyser, equipped with a BLC as described in Sect. 2.2.1, diluted in zero air through a range of mixing ratios. The resulting mixing ratio recorded by the analyser is presented in the following sections. Figure 2 shows that the artifact NO_2 signal is proportional to increasing PAN mixing ratios. An artificial signal corresponding to 8 to 25 % of the initial PAN mixing ratio was generated.

The percentage conversion of PAN to NO_2 is on average highest at the lowest converter efficiency and vice versa. Potential reasons for this effect are addressed in Sect. 3.6.

3.2 Standard BLC and laboratory NO_x analyser in switching mode

Figure 3 shows the artifact NO_2 signal resulting from PAN using the same three BLC units operated in switching mode (40 % duty cycle). The percentage PAN conversion observed is lower in all cases than in the corresponding constant mode. This is likely due to the lower lamp temperature as a result of operating only 40 % of the time. The relationship between conversion efficiency and signal are not as clearly evident here as for constant mode operation (Fig. 2). It is possible that the greater variation in the measurement due to the lower amounts of NO_2 produced obscured any trend, however it is clear that there is still a significant proportion of PAN measured as NO_2 ; an average of 5.8 %.

3.3 Inlet residence time effects

It is not clear from either Fig. 2 or 3 whether the PAN decomposition occurs within the BLC exclusively or within the inlet of the system, as has been claimed previously (Fehsenfeld et al., 1987). Previous studies (Fehsenfeld et al., 1990; Ridley et al., 1988; Sadanaga et al., 2010) have also reported a small PAN interference with photolytic converters, while some found the contribution to the NO_2 signal from PAN to be negligible (Ryerson et al., 2000).

Others (Val Martin et al., 2008) acknowledge the possibility for interference and estimate a small (2 to 4 pptv) positive bias. The photolytic converter designs in these studies vary greatly in their implementation and do not have the same ubiquity as BLCs used here, i.e. within the GAW network (Penkett et al., 2011).

Table 2 demonstrates that the residence time of PAN within the inlet does not affect the signal arising from PAN decomposition in our system. This rules out any significant contribution from PAN decomposition in the inlet to any artifact signal. The inlet in this case consists of ~ 2.7 m 1/4 inch PFA tubing shielded from light and held at 20 °C. In other applications, for example if the inlet is heated, contaminated, or has a very long residence time, it is quite possible that significant PAN decomposition occurs.

From these experiments it is evident that a significant NO₂ signal is observed when sampling PAN diluted in zero air. The signal seen corresponds to around 8 to 25% of the PAN supplied which represents a significant interference. The possibility of thermal decomposition within the inlet was ruled out.

3.4 High powered and actively cooled photolytic NO₂ converter

Figure 4 shows the difference in NO₂ signal between the cooled and uncooled high powered BLC described in Sect. 2.2.2. In all of the cooled cases the NO₂ measured was significantly lower than in the uncooled case; this accounts for any increased artifact (the signal recorded when sampling zero air) in the uncooled case. The conversion efficiency was 93 % for NO₂ → NO.

The effect of actively cooling the BLC lamps is significant as apparent in the much lower NO₂ concentrations measured whilst sampling a range of PAN mixing ratios (Fig. 4). It is therefore evident that there is a significant effect of cooling the UV-LEDs which acts to mitigate any signal arising from PAN.

3.5 Possible photolytic interferences of BLCs

There exists potential for photolytic interferences in photolytic converters e.g. HONO depending on their spectral overlap. Here we investigate this possibility with BLCs by taking the spectral output of a range of LED units against the absorption cross-sections of various atmospheric compounds.

Spectral radiograms of the UV-LED elements of standard BLCs were obtained using an Ocean Optics QE65000 spectral radiometer coupled to a 2π quartz collector. The spectrometer and collector optics were calibrated using an NIST traceable light source (OL FEL-A, Gooch and Housego) and ultra-linear power supply (OL 83A, Gooch and Housego). The light source is a 1000 W quartz-halogen tungsten coiled-coil filament lamp with spectral irradiance standard F-1128. The lamp was operated at 8 Amps DC (125 V), with the lamp-collector distance fixed at 50 cm. Calibration was carried out in a light sealed chamber. Spectra of the BLC UV-LED lamps were taken within the same light-proof chamber with the same distance between the lamp and collector.

Figure 5 shows the spectral emission of six different BLC UV-LED units. These units ranged in age from new to nearing the end of their service life i.e. the conversion efficiency of the whole BLC unit had fallen below acceptable limits. As the LED units age, the relative intensity of their outputs declines, this decrease in intensity can be due to dimming of the overall output, or failure of individual array elements determined by visual inspection during operation. It should be pointed out however, that the light intensity of the UV-LEDs is not directly proportional to the NO_2 conversion efficiency of the complete whole BLC. Rather, the conversion efficiency is strongly dictated by the condition of the reflective Teflon-like cavity. For example, disabling one of the two lamps in a BLC does not reduce the conversion efficiency by half, but by a much smaller percentage. Additionally, replacing the UV-LED elements of a converter whose conversion efficiency has dropped below 30 % with new lamps will not lead to a recovery of the conversion. Scrupulous cleaning of the reflective cavity with solvent and mild abrasion of the surface will however recover the conversion efficiency considerably. This is because Teflon-like block is a bulk reflector, that is, the UV penetrates

up to ~ 1 cm into the material. It is this reflective property that makes most efficient use of the light and achieves high conversion efficiency at low residence times. Adsorption of any UV absorbing material on the surface reduces the reflectivity dramatically. Additionally, the Teflon block is somewhat porous and so contaminants may penetrate into the bulk (or at least below the surface). Solvent may remove most of the contaminants (though strong solvents can damage the block), however those which have moved below the surface can only be removed by removing the layer of Teflon contaminated. The porosity also gives rise to the artifact NO_2 signal as new material off-gasses (as can other surfaces e.g. LED die). Sample gas may also diffuse into, and out of, the bulk very slowly giving a small memory effect as NO_x and NO_y exchange with the sample stream.

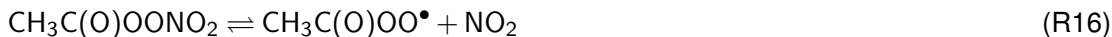
Figure 6 depicts the absorption cross sections of atmospheric nitrogen compounds (Sander et al, 2011) against the measured spectral output of UG5 UV-passing filter glass (Schott, 1997) used in lamp-type photolytic converter (PLC) optics e.g. Eco Physics AG PLC 760, and the averaged measured spectral output of six individual BLC UV-LED arrays of varying running hours. Also shown is the NO_2 quantum yield (Gardner, 1987; Koepke et al., 2010). It can be discerned that the UV-LED output overlaps fully with the NO_2 absorption band and the NO_2 quantum yield and is therefore photon efficient. It is also shown that there is minimal overlap with HONO and no overlap in the spectrum at all with PAN. It has been shown (Carbajo and Orr-Ewing, 2010; Talukdar et al., 1997) that there is no overlap either with methyl, ethyl or isopropyl nitrate – methyl nitrate being a minor impurity in PAN synthesis. There is only very minor overlap in the PLC optics spectrum with PAN, methyl ethyl, and isopropyl nitrate. PLC optics exhibit a great deal of overlap with HONO which the UV-LEDs do not. Both systems suffer some overlap with NO_3 radicals and BrONO_2 , more so in the case of PLC optics than for UV-LEDs. It is evident that PAN is unable to be photolysed in a BLC, nor other types of photolytic converter, due to the narrow spectral output of UV not having overlap with the PAN absorption spectrum. Other species such as HONO, BrONO_2 , and NO_3 radicals may constitute a photolytic interference.

3.6 Possible thermal interferences in BLCs

The thermal and electronic characteristics of the standard BLC lamps were found in bench tests and are summarized in Table 3. Each lamp was run constantly whilst recording the surface temperature and power draw of the light emitting element. The surface temperature was recorded once a stable maximum had been reached and maintained for at least 10 min – representative of using a BLC in constant mode. The ambient temperature during the experiments was 20 °C.

Table 3 describes the power draw and surface temperature of three BLC UV-LED lamp pairs measured during tests, along with their NO₂ → NO convertor efficiencies when assembled as a complete BLC. The surface temperature of the individual lamps correlate positively with the power drawn by each lamp ($R^2 = 0.96$) and indeed with output intensity (Fig. 2), but with each lamp pair there is only weak correlation ($R^2 = 0.43$) between converter efficiency and temperature. It is worth noting that the power consumption is a combination of the light output, heat dissipation, and power to the cooling fan. It is clear however that the temperature experienced by the sample gas within the NO₂ converter is significantly above ambient. In fact, the entire NO₂ conversion cavity is heated by the lamps leading to external temperatures of the converter of between 34 and 45 °C.

It is known that the major product from thermal decomposition of PAN is NO₂; Reaction (R16) (Roumelis and Glavas, 1992; Tuazon et al., 1991). The NO₂ produced thermally within the converter may then be photolysed to NO and thus be measured as NO_x and attributed to atmospheric NO₂.



A model of the gas phase thermal decomposition of PAN over a range of temperatures within the BLC with a residence time of 0.96 s is shown in Fig. 7. The model run was conducted in FACSIMILE kinetic modelling software (MCPA Software Ltd.) using rate constants from IUPAC Evaluated Kinetic Data (Atkinson et al., 2006).

The model output indicates that measurable PAN decomposition to NO₂ occurs above ~ 50 °C. At the maximum LED surface temperature recorded (80 °C) the model predicts

~ 30% decomposition of PAN to NO₂. However, as only the two UV-LED lamps are at such an elevated temperature we can expect a temperature gradient/heating rate within the BLC so that the average temperature seen by the sample gas over the 0.96 s residence is somewhat lower. We assume that only gas phase decomposition occurs, rather than any surface enhanced heterogeneous process, however as the BLC has; Teflon, stainless steel, rubber, conformal coating etc. contacting the sample gas (some of which maybe heated to an extent) it is a possibility. Ryerson et al. (2000) found no measurable PAN decomposition on the quartz surface of their converter. It is expected that in a switching mode with only 40% duty cycle of the lamps, their surface temperature would be lower also. This is borne out when using the external surface temperature of the BLC as a proxy – the temperature was lower in switching mode than in constant mode for the same conversion efficiency. It is shown more clearly in the inset that an average temperature of 60°C would cause a 4.6% decomposition of PAN and account for the NO₂ measured during experiments with the standard BLCs. Therefore, together with the spectral measurements reported in Sect. 3.5, it seems highly unlikely that the source of the artifact signal is through direct photolysis of PAN, leaving thermal decomposition, modelled in Fig. 7, the remaining explanation.

In Sect. 3.1 the percentage conversion of PAN to NO₂ was found to be, on average, highest at the lowest converter efficiency and vice versa. The fact that the converter temperatures are very similar at different converter efficiencies (Table 3) suggests that the percentage of PAN thermally dissociated in each case is similar. Explanation for the inverse relationship between percentage conversion of PAN to NO and conversion efficiency (Fig. 2) lies in the way that the NO₂ concentration is derived, which is an inverse function of the assumed conversion efficiency as in Eq. (2) where converter efficiency is expressed fractionally. If in fact the conversion efficiency of PAN to NO in the converter was not related to the measured NO₂ to NO conversion efficiency but instead a constant value, then the apparent relationship between CE and % conversion would disappear. This explanation is consistent with the fact that when the average conversion percentage in Fig. 2 is normalized to conversion efficiency, the percentage for the three BLCs is remarkably similar

(Table 4) with the average PAN decomposition of 4.6% needed to produce the spurious signal observed.

Above a threshold temperature of 25 °C, the NO₂ formed in Reaction (R16) may be vibrationally excited (likely NO₂(²A₁)) through the dissipating of internal energy from the parent PAN molecule (MaNO_xy et al., 1995), this NO₂^{*} is then more readily photolysed to NO within the BLC than ground state NO₂. The discussion above suggests that a similar proportion of the NO₂ evolved from thermal dissociation of PAN is converted to NO within the BLC leading to the apparent inverse correlation between conversion efficiency and PAN “artifact”. Consequently, the lower NO₂ → NO conversion efficiency of a BLC, the greater the positive error in NO₂ when PAN is present.

4 Atmospheric implications

We have shown that a significant proportion of PAN can be decomposed under the normal operating conditions of a BLC equipped NO chemiluminescence instrument leading to a spurious increase in measured NO₂ of 8 to 25 % of the PAN supplied. The UV-LED light source was found to reach a temperature of 56 to 80 °C in normal operation, with the surface temperature correlating positively with power draw and output intensity. The elevated temperature of the UV-LEDs causes a positive bias in NO₂ by thermal decomposition of PAN.

The positive bias in NO₂ measurements by NO chemiluminescence using BLCs has implications for remote background sites. Figure 8 shows the thermal decomposition profiles of many common NO_y species. Whereas only a small fraction of PAN is found to convert to NO₂ at the operating temperatures (~ 5 % at 60 °C) of the instrument, a number of more thermally labile compounds exist.

The degree of gas phase thermal decomposition within the instrument will depend upon the thermal profile of the air ($T(t)$) as it passes through the instrument. This can be parameterized as a mixing timescale (τ s) for temperature from the ambient temperature (T_0) to

that of the BLC (T_{BLC}) as in Eq. (4).

$$T(t) = T_0 + (T_{\text{BLC}} - T_0) \exp\left(-\frac{t}{\tau}\right) \quad (4)$$

The rate at which thermal equilibrium is reached within the cell, τ , is calculated as 0.42 s from the observed PAN decomposition of 4.6%, at 20 °C ambient temperature, a BLC temperature of 75 °C and a 1 s residence time. This allows calculation of the potential interference from other thermally labile NO_y compounds.

Given a 1st order loss of the PAN like compound and a temperature profile within in the instrument as described in 4 we have 5:

$$\frac{d[\text{PAN}]}{dt} = -k(T)[\text{PAN}] = -k(t)[\text{PAN}] \quad (5)$$

Given the laboratory observations of the temperature dependence of the rate constant (typically $k(T) = A \exp(-B/T)$), and the parameterized temperature within the instrument ($T(t)$), the fraction of the compounds that will have decomposed can be found by numerical integration.

Figure 9 uses output from the GEOS-Chem model (version 9.2, <http://www.geos-chem.org>, Bey et al., 2001) run at $2^\circ \times 2.5^\circ$ resolution, plus updates described in Sherwen et al. (2016), to provide an estimate of the interference on NO_2 from the decomposition of NO_y species within a BLC photolytic converter. The species used for this analysis are: PAN; MPAN; PPN; IONO_2 ; BrONO_2 ; N_2O_5 ; $\text{CH}_3\text{O}_2\text{NO}_2$, HO_2NO_2 . Thermal decomposition information are taken from IUPAC evaluated kinetic data (Atkinson et al., 2003, 2006, 2007). Interferences are calculated for each month of a one year simulation and the maximum value shown. The estimate assumes a BLC conversion efficiency of 100 % $\text{NO}_2 \rightarrow \text{NO}$ and thus does not include the extra signal from the photolysis of $\text{NO}_2^* \rightarrow \text{NO}$ with converters where conversion is less than unity – in this case a multiplying factor exists.

Figure 9 shows that in extreme circumstances NO_2 may be over-reported by many hundreds of percent. These are in regions that typically have low NO_x concentrations and are

cold (polar), or in the upper troposphere. Here, the concentration of compounds such as PAN and HO₂NO₂ are high relative to NO_x and it is not surprising that thermal decomposition can have an impact. Upper tropospheric over estimates of NO₂ concentrations could be as high as 150 pptv, which we find due to CH₃O₂NO₂ abundance, which has previously been identified as a possible interference in NO₂ measurement by LIF and chemiluminescence (Browne et al., 2011; Nault et al., 2015).

The NO₂ bias shown in Fig. 9 impacts the modelled Leighton ratio. In Fig. 10 the model is sampled every daylight hour for every surface grid box for the month of March. The calculation shown in red is the Leighton ratio calculated from the modelled concentrations of NO, NO₂, jNO₂, O₃, T, HO₂, RO₂, BrO and IO. The model values are in general close to 1. In blue the same calculation is performed but including the interferences on the NO₂ channel. The instrumental decomposition of NO_y over a range of BLC lamp temperatures between 20 and 95 °C are shown (described by τ of 0.42 s and a residency time of 1 s). Here there are significant interferences.

As shown in Fig. 10 the Leighton ratio can be extremely perturbed from what would be predicted for NO₂ converters which operate above ambient temperature. This is especially true in low NO_x environments.

Unusual Leighton relationships have been seen in a range of previous studies (Bauguitte et al., 2012; Cantrell et al., 2003; Frey et al., 2013, 2015; Griffin et al., 2007; Hosaynali Beygi et al., 2011; Kanaya et al., 2007; Yang et al., 2004) leading to either hypothesizing (a) an unknown, unmeasured, selective oxidant “compound X” or, (b) theoretical mechanisms by which NO is converted to NO₂ which may be accounted for, in part, by a previously unaccounted for instrument bias our study has suggested. It is noteworthy that the studies of Bauguitte, Cantrell, Frey, Griffin, Hosaynali Beygi, Kanaya, and Yang were all in locations where we predict a significant interference (indicated on Fig. 9), impacting on the observed Leighton relationship and complicating interpretation.

5 Conclusions

Measurements of NO_2 collected using some types of photolytic converter and chemiluminescence systems may be significantly biased in low NO_x environments. Thermal decomposition of NO_y species within the NO_2 converter produces spuriously high readings; this is especially true in pristine environments and at high elevations where the NO_y to NO_x ratio may be high. Over-reporting of NO_2 has been shown to lead to apparent gaps in oxidation chemistry which cannot be explained with any available measurements. This has led to the theorization of an unknown “compound X ” which selectively oxidizes NO to NO_2 , however this is likely anomalous and simply due to errors in NO_2 determination.

Investigators wishing to determine Leighton ratios, especially with the BLC/ NO chemiluminescence technique, would be advised to characterise their instruments thoroughly with respect to interference from thermally decomposing NO_y species. A convenient method for this would be with a pure PAN source, or any other readily available NO_y species.

In order to mitigate overestimation of the NO_2 mixing ratio by thermally dissociating PAN and other compounds it is imperative to avoid heating of the sample above ambient. This can be achieved by separating the gas flow from contact with the UV emitting elements, and by cooling the photolysis cell. Reducing the residence time of the sample gas within an instrument where it may not be possible to maintain ambient temperature of the sample is an alternative i.e. where the ambient temperature is unfeasibly low. This can be achieved by operating at reduced inlet pressure, with the additional benefit of faster response time. It is desirable to have the highest possible $\text{NO}_2 \rightarrow \text{NO}$ conversion efficiency, i.e. unity, to minimise uncertainty in NO_2 and to remove any multiplying effect of more easily photolysable vibrationally excited NO_2 . It would also seem prudent that the sample gas should contact only chemically inert, and non-porous materials in order to mitigate any heterogeneous processes or memory effect; quartz being an ideal material for photolysis cells.

Acknowledgements. The authors would like to express their gratitude to Stephane Bauguitte of FAAM for their scientific discussion, and Lisa Whalley of Leeds for the PAN generator and spectral radiometer/calibration equipment. The financial support of NCAS, the National Centre for At-

ospheric Science, and of NERC, the Natural Environmental Research Council for supporting the studentship of Chris Reed is gratefully acknowledged.

References

- Ainsworth, E. A., Yendrek, C. R., Sitch, S., Collins, W. J., and Emberson, L. D.: The effects of tropospheric ozone on net primary productivity and implications for climate change, *Annu. Rev. Plant Biol.*, 63, 637–661, doi:10.1146/annurev-arplant-042110-103829, 2012.
- Ashmore, M. R.: Assessing the future global impacts of ozone on vegetation, *Plant Cell Environ.*, 28, 949–964, doi:10.1111/j.1365-3040.2005.01341.x, 2005.
- Atkinson, R., Baulch, D. L., Cox, R. A., Crowley, J. N., Hampson, R. F., Hynes, R. G., Jenkin, M. E., Rossi, M. J., and Troe, J.: Evaluated kinetic and photochemical data for atmospheric chemistry: Volume I – gas phase reactions of O_x , HO_x , NO_x and SO_x species, *Atmos. Chem. Phys.*, 4, 1461–1738, doi:10.5194/acp-4-1461-2004, 2004.
- Atkinson, R., Baulch, D. L., Cox, R. A., Crowley, J. N., Hampson, R. F., Hynes, R. G., Jenkin, M. E., Rossi, M. J., Troe, J., and IUPAC Subcommittee: Evaluated kinetic and photochemical data for atmospheric chemistry: Volume II – gas phase reactions of organic species, *Atmos. Chem. Phys.*, 6, 3625–4055, doi:10.5194/acp-6-3625-2006, 2006.
- Atkinson, R., Baulch, D. L., Cox, R. A., Crowley, J. N., Hampson, R. F., Hynes, R. G., Jenkin, M. E., Rossi, M. J., and Troe, J.: Evaluated kinetic and photochemical data for atmospheric chemistry: Volume III – gas phase reactions of inorganic halogens, *Atmos. Chem. Phys.*, 7, 981–1191, doi:10.5194/acp-7-981-2007, 2007.
- Bauguitte, S. J.-B., Bloss, W. J., Evans, M. J., Salmon, R. A., Anderson, P. S., Jones, A. E., Lee, J. D., Saiz-Lopez, A., Roscoe, H. K., Wolff, E. W., and Plane, J. M. C.: Summertime NO_x measurements during the CHABLIS campaign: can source and sink estimates unravel observed diurnal cycles?, *Atmos. Chem. Phys.*, 12, 989–1002, doi:10.5194/acp-12-989-2012, 2012.
- Bridier, I., Caralp, F., Loirat, H., Lesclaux, R., Veyret, B., Becker, K. H., Reimer, A., and Zabel, F.: Kinetic and theoretical studies of the reactions $CH_3C(O)O_2 + NO_2 + M \rightleftharpoons CH_3C(O)O_2 + M$ between 248 and 393 K and between 30 and 760 torr, *J. Phys. Chem.*, 95, 3594–3600, doi:10.1021/j100162a031, 1991.
- Browne, E. C., Perring, A. E., Wooldridge, P. J., Apel, E., Hall, S. R., Huey, L. G., Mao, J., Spencer, K. M., St. Clair, J. M., Weinheimer, A. J., Wisthaler, A., and Cohen, R. C.: Global and re-

- gional effects of the photochemistry of $\text{CH}_3\text{O}_2\text{NO}_2$: evidence from ARCTAS, *Atmos. Chem. Phys.*, 11, 4209–4219, doi:10.5194/acp-11-4209-2011, 2011.
- Brown, S. S., Dibb, J. E., Stark, H., Aldener, M., Vozella, M., Whitlow, S., Williams, E. J., Lerner, B. M., Jakoubek, R., Middlebrook, A. M., DeGouw, J. A., Warneke, C., Goldan, P. D., Kuster, W. C., Angevine, W. M., Sueper, D. T., Quinn, P. K., Bates, T. S., Meagher, J. F., Fehsenfeld, F. C., and Ravishankara, A. R.: Nighttime removal of NO_x in the summer marine boundary layer, *Geophys. Res. Lett.*, 31, L07108, doi:10.1029/2004GL019412, 2004.
- Brown, S. S., Osthoff, H. D., Stark, H., Dubé, W. P., Ryerson, T. B., Warneke, C., DeGouw, J. A., Wollny, A. G., Parrish, D. D., Fehsenfeld, F. C., and Ravishankara, A. R.: Aircraft observations of daytime NO_3 and N_2O_5 and their implications for tropospheric chemistry, *J. Photochem. Photobiol. A: Chemistry*, 176, 270–278, doi:10.1016/j.jphotochem.2005.10.004, 2005.
- Buhr, M.: Measurement of NO_2 in ambient air using a solid-state photolytic converter, in: *Symposium on Air Quality Measurement Methods and Technology 2004*, 20–22 April 2004, 165–171, Cary, NC, USA, 2004.
- Buhr, M.: Solid-State Light Source Photolytic Nitrogen Dioxide Converter, US 7238328 B2, 3 July 2007.
- Cantrell, C. A., Shetter, R. E., Calvert, J. G., Eisele, F. L., Williams, E., Baumann, K., Brune, W. H., Stevens, P. S., and Mather, J. H.: Peroxy radicals from photostationary state deviations and steady state calculations during the Tropospheric OH Photochemistry Experiment at Idaho Hill, Colorado, 1993, *J. Geophys. Res.*, 102, 6369, doi:10.1029/96JD01703, 1997.
- Cantrell, C. A., Mauldin, L., Zondlo, M., Eisele, F. L., Kosciuch, E., Shetter, R. E., Lefer, B., Hall, S., Campos, T. L., Ridley, B., Walega, J. G., Fried, A., Wert, B., Flocke, F. M., Weinheimer, A. J., Hannigan, J., Coffey, M., Atlas, E., Stephens, S., Heikes, B. G., Snow, J., Blake, D. R., Blake, N., Katzenstein, A., Lopez, J., Browell, E. V., Dibb, J. E., Scheuer, E., Seid, G., and Talbot, R. W.: Steady state free radical budgets and ozone photochemistry during TOPSE, *J. Geophys. Res.*, 108, 8361, doi:10.1029/2002JD002198, 2003.
- Carbajo, P. G. and Orr-Ewing, A. J.: NO_2 quantum yields from ultraviolet photodissociation of methyl and isopropyl nitrate., *Phys. Chem. Chem. Phys.*, 12, 6084–6091, doi:10.1039/c001425g, 2010.
- Carslaw, D. C.: Evidence of an increasing NO_2/NO_x emissions ratio from road traffic emissions, *Atmos. Environ.*, 39, 4793–4802, doi:10.1016/j.atmosenv.2005.06.023, 2005.
- Clemittshaw, K. C., Carpenter, L. J., Penkett, S. A. and Jenkin, M. E.: A calibrated peroxy radical chemical amplifier for ground-based tropospheric measurements, *J. Geophys. Res.*, 102, 25405–25416, doi:10.1029/97JD01902, 1997.

- Clough, P. N. and Thrush, B. A.: Mechanism of chemiluminescent reaction between nitric oxide and ozone, *Trans. Faraday Soc.*, 63, 915–925 doi:10.1039/TF9676300915, 1967.
- Clyne, M. A. A., Thrush, B. A., and Wayne, R. P.: Kinetics of the chemiluminescent reaction between nitric oxide and ozone, *Trans. Faraday Soc.*, 60, 359–370, doi:10.1039/TF9646000359, 1964.
- Crutzen, P. J.: The role of NO and NO₂ in the chemistry of the troposphere and stratosphere, *Annu. Rev. Earth Planetary Sci.*, 7, 443–472, doi:10.1146/annurev.ea.07.050179.002303, 1979.
- Dalsøren, S. B. and Isaksen, I. S. A.: CTM study of changes in tropospheric hydroxyl distribution 1990–2001 and its impact on methane, *Geophys. Res. Lett.*, 33, L23811, doi:10.1029/2006GL027295, 2006.
- Dari-Salisburgo, C., Di Carlo, P., Giammaria, F., Kajii, Y., and D’Altorio, A.: Laser induced fluorescence instrument for NO₂ measurements: observations at a central Italy background site, *Atmos. Environ.*, 43, 970–977, doi:10.1016/j.atmosenv.2008.10.037, 2009.
- Day, D. A., Wooldridge, P. J., Dillon, M. B., Thornton, J. A., and Cohen, R. C.: A thermal dissociation laser-induced fluorescence instrument for in situ detection of NO₂, peroxy nitrates, alkyl nitrates, and HNO₃, *J. Geophys. Res.*, 107, ACH 4-1–ACH 4-14, doi:10.1029/2001JD000779, 2002.
- Dentener, F. J. and Crutzen, P. J.: Reaction of N₂O₅ on tropospheric aerosols: impact on the global distributions of NO_x, O₃, and OH, *J. Geophys. Res.*, 94, 7149–7163, doi:10.1029/92JD02979, 1993.
- Di Carlo, P., Aruffo, E., Busilacchio, M., Giammaria, F., Dari-Salisburgo, C., Biancofiore, F., Visconti, G., Lee, J., Moller, S., Reeves, C. E., Bauguitte, S., Forster, G., Jones, R. L., and Ouyang, B.: Aircraft based four-channel thermal dissociation laser induced fluorescence instrument for simultaneous measurements of NO₂, total peroxy nitrate, total alkyl nitrate, and HNO₃, *Atmos. Meas. Tech.*, 6, 971–980, doi:10.5194/amt-6-971-2013, 2013.
- Drummond, J. W., Volz, A., and Ehhalt, D. H.: An optimized chemiluminescence detector for tropospheric NO measurements, *J. Atmos. Chem.*, 2, 287–306, doi:10.1007/BF00051078, 1985.
- Dunlea, E. J., Herndon, S. C., Nelson, D. D., Volkamer, R. M., San Martini, F., Sheehy, P. M., Zahniser, M. S., Shorter, J. H., Wormhoudt, J. C., Lamb, B. K., Allwine, E. J., Gaffney, J. S., Marley, N. A., Grutter, M., Marquez, C., Blanco, S., Cardenas, B., Retama, A., Ramos Villegas, C. R., Kolb, C. E., Molina, L. T., and Molina, M. J.: Evaluation of nitrogen dioxide chemiluminescence monitors in a polluted urban environment, *Atmos. Chem. Phys.*, 7, 2691–2704, doi:10.5194/acp-7-2691-2007, 2007.
- Fehsenfeld, F. C., Dickerson, R. R., Hobler, G., Luke, W. T., Nunnermacker, L. J., Roberts, J. M., Curran, C. M., Eubank, C. S., Fahey, D. W., Mindplay, P. C., and Pickering, K. E.: A ground-based

- intercomparison of NO, NO_x, and NO_y measurement techniques, *J. Geophys. Res.*, 92, 710–722, doi:10.1029/JD092iD12p14710, 1987.
- Fehsenfeld, F. C., Drummond, J. W., Roychowdhury, U. K., Galvin, P. J., Williams, E. J., Burr, M. P., Parrish, D. D., Hobler, G., Langford, A. O., Calvert, J. G., Ridley, B. A., Heikes, B. G., Kok, G. L., Shetler, J. D., Walega, J. G., Elsworth, C. M., and Mohnen, V. A.: Intercomparison of NO₂ measurement techniques, *J. Geophys. Res.*, 95, 3579–3597, doi:10.1029/JD095iD04p03579, 1990.
- Fischer, E. V., Jacob, D. J., Yantosca, R. M., Sulprizio, M. P., Millet, D. B., Mao, J., Paulot, F., Singh, H. B., Roiger, A., Ries, L., Talbot, R. W., Dzepina, K., and Pandey Deolal, S.: Atmospheric peroxyacetyl nitrate (PAN): a global budget and source attribution, *Atmos. Chem. Phys.*, 14, 2679–2698, doi:10.5194/acp-14-2679-2014, 2014.
- Fischer, G. and Nwankwoala, A. U.: A spectroscopic study of the thermal decomposition of peroxyacetyl nitrate (PAN), *Atmos. Environ.*, 29, 3277–3280, doi:10.1016/1352-2310(95)00252-T, 1995.
- Flocke, F. M., Weinheimer, A. J., Swanson, A. L., Roberts, J. M., Schmitt, R., and Shertz, S.: On the Measurement of PANs by Gas Chromatography and Electron Capture Detection, *Journal of Atmospheric Chemistry*, 52, 19–43 doi:10.1007/s10874-005-6772-0, 2005.
- Fontijn, A., Sabadell, A. J., and Ronco, R. J.: Homogeneous chemiluminescent measurement of nitric oxide with ozone. Implications for continuous selective monitoring of gaseous air pollutants, *Anal. Chem.*, 42, 575–579, doi:10.1021/ac60288a034, 1970.
- Frey, M. M., Brough, N., France, J. L., Anderson, P. S., Traulle, O., King, M. D., Jones, A. E., Wolff, E. W., and Savarino, J.: The diurnal variability of atmospheric nitrogen oxides (NO and NO₂) above the Antarctic Plateau driven by atmospheric stability and snow emissions, *Atmos. Chem. Phys.*, 13, 3045–3062, doi:10.5194/acp-13-3045-2013, 2013.
- Frey, M. M., Roscoe, H. K., Kukui, A., Savarino, J., France, J. L., King, M. D., Legrand, M., and Preunkert, S.: Atmospheric nitrogen oxides (NO and NO₂) at Dome C, East Antarctica, during the OPALE campaign, *Atmos. Chem. Phys.*, 15, 7859–7875, doi:10.5194/acp-15-7859-2015, 2015.
- Gardner, E. P., Sperry, P. D., and Calvert, J. G.: Primary quantum yields of NO₂ photodissociation, *J. Geophys. Res.*, 92, 6642–6652, doi:10.1029/JD092iD06p06642, 1987.
- Griffin, R. J., Beckman, P. J., Talbot, R. W., Sive, B. C., and Varner, R. K.: Deviations from ozone photostationary state during the International Consortium for Atmospheric Research on Transport and Transformation 2004 campaign: Use of measurements and photochemical modeling to assess potential causes, *J. Geophys. Res.*, 112, D10S07, doi:10.1029/2006JD007604, 2007.

- Grosjean, D., Harrison, J.: Response of chemiluminescence NO_x analyzers and ultraviolet ozone analyzers to organic air pollutants, *Environ. Sci. Technol.*, 1985, 19, pp 862–865, doi: 10.1021/es00139a016, 1985.
- Hollaway, M. J., Arnold, S. R., Challinor, A. J., and Emberson, L. D.: Intercontinental trans-boundary contributions to ozone-induced crop yield losses in the Northern Hemisphere, *Biogeosciences*, 9, 271–292, doi:10.5194/bg-9-271-2012, 2012.
- Hosaynali Beygi, Z., Fischer, H., Harder, H. D., Martinez, M., Sander, R., Williams, J., Brookes, D. M., Monks, P. S., and Lelieveld, J.: Oxidation photochemistry in the Southern Atlantic boundary layer: unexpected deviations of photochemical steady state, *Atmos. Chem. Phys.*, 11, 8497–8513, doi:10.5194/acp-11-8497-2011, 2011.
- Huntrieser, H., Schlager, H., Roiger, A., Lichtenstern, M., Schumann, U., Kurz, C., Brunner, D., Schwierz, C., Richter, A., and Stohl, A.: Lightning-produced NO_x over Brazil during TROCCINOX: airborne measurements in tropical and subtropical thunderstorms and the importance of mesoscale convective systems, *Atmos. Chem. Phys.*, 7, 2987–3013, doi:10.5194/acp-7-2987-2007, 2007.
- Kanaya, Y., Tanimoto, H., Matsumoto, J., Furutani, H., Hashimoto, S., Komazaki, Y., Tanaka, S., Yokouchi, Y., Kato, S., Kajii, Y., and Akimoto, H.: Diurnal variations in H₂O₂, O₃, PAN, HNO₃ and aldehyde concentrations and NO/NO₂ ratios at Rishiri Island, Japan: potential influence from iodine chemistry, *Sci. Total Environ.*, 376, 185–197, doi:10.1016/j.scitotenv.2007.01.073, 2007.
- Kelly, T. J., Stedman, D. H., Ritter, J. A., and Harvey, R. B.: Measurements of oxides of nitrogen and nitric acid in clean air, *J. Geophys. Res.*, 85, 7417–7425, doi:10.1029/JC085iC12p07417, 1980.
- Kleindienst, T. E.: Recent developments in the chemistry and biology of peroxyacetyl nitrate, *Res. Chem. Intermed.*, 20, 335–384, doi:10.1163/156856794X00379, 1994.
- Kley, D., Drummond, J. W., McFarland, M., and Liu, S. C.: Tropospheric profiles of NO_x, *J. Geophys. Res.*, 86, 3153–3161, doi:10.1029/JC086iC04p03153, 1981.
- Koepke, P., Garhammer, M., Hess, M., and Roeth, E.-P.: NO₂ photolysis frequencies in street canyons, *Atmos. Chem. Phys.*, 10, 7457–7466, doi:10.5194/acp-10-7457-2010, 2010.
- Lee, J. D., Moller, S. J., Read, K. A., Lewis, A. C., Mendes, L., and Carpenter, L. J.: Year-round measurements of nitrogen oxides and ozone in the tropical North Atlantic marine boundary layer, *J. Geophys. Res.*, 114, D21302, doi:10.1029/2009JD011878, 2009.
- Leighton, P. A.: *Photochemistry of Air Pollution*, Academic Press, University of Michigan, Ann Arbor, Michigan, USA, 1961.

- Lelieveld, J., Dentener, F. J., Peters, W., and Krol, M. C.: On the role of hydroxyl radicals in the self-cleansing capacity of the troposphere, *Atmos. Chem. Phys.*, 4, 2337–2344, doi:10.5194/acp-4-2337-2004, 2004.
- Levy II, H.: Photochemistry of the lower troposphere, *Planet. Space Sci.*, 20, 919–935, doi:10.1016/0032-0633(72)90177-8, 1972.
- Mannschreck, K., Gilge, S., Plass-Duelmer, C., Fricke, W., and Berresheim, H.: Assessment of the applicability of NO-NO₂-O₃ photostationary state to long-term measurements at the Hohenpeisenberg GAW Station, Germany, *Atmos. Chem. Phys.*, 4, 1265-1277, doi:10.5194/acp-4-1265-2004, 2004.
- Matsumoto, J. and Kajii, Y.: Improved analyzer for nitrogen dioxide by laser-induced fluorescence technique, *Atmos. Environ.*, 37, 4847–4851, doi:10.1016/j.atmosenv.2003.08.023, 2003.
- Matsumoto, J., Hirokawa, J., Akimoto, H., and Kajii, Y.: Direct measurement of NO₂ in the marine atmosphere by laser-induced fluorescence technique, *Atmos. Environ.*, 35, 2803–2814, doi:10.1016/S1352-2310(01)00078-4, 2001.
- Mauzerall, D. L., Sultan, B., Kim, N., and Bradford, D. F.: NO emissions from large point sources: variability in ozone production, resulting health damages and economic costs, *Atmos. Environ.*, 39, 2851–2866, doi:10.1016/j.atmosenv.2004.12.041, 2005.
- Mazely, T. L., Friedl, R. R., and Sander, S. P.: Production of NO₂ from photolysis of peroxyacetyl nitrate, *J. Phys. Chem.*, 99, 8162–8169, doi:10.1021/j100020a044, 1995.
- McClenny, W. A., Williams, E. J., Cohen, R. C., and Stutz, J.: Preparing to Measure the Effects of the NO_x SIP Call– Methods for Ambient Air Monitoring of NO, NO₂, NO_y, and Individual NO_z Species, *J. Air & Waste Manage. Assoc.* 5, 52, 542–562, doi:110.1080/10473289.2002.10470801, 2002
- Meyrahn, H., Helas, G., and Warneck, P.: Gas chromatographic determination of peroxyacetyl nitrate: two convenient calibration techniques, *J. Atmos. Chem.*, 5, 405–415, doi:10.1007/BF00113903, 1987.
- Mills, G. P., Sturges, W. T., Salmon, R. A., Bauguitte, S. J.-B., Read, K. A., and Bandy, B. J.: Seasonal variation of peroxyacetylnitrate (PAN) in coastal Antarctica measured with a new instrument for the detection of sub-part per trillion mixing ratios of PAN, *Atmos. Chem. Phys.*, 7, 4589–4599, doi:10.5194/acp-7-4589-2007, 2007.
- Moore, R. M. and Blough, N. V.: A marine source of methyl nitrate, *Geophys. Res. Lett.*, 29, 27-1–27-4, doi:10.1029/2002GL014989, 2002.
- Moxim, W. J., Levy II, H. and Kasibhalta, P. S.: Simulated global tropospheric PAN: Its transport and impact on NO_x, *J. Geophys. Res.*, 101, 12621–12638, doi:10.1029/96JD00338, 1996.

- Nault, B. A., Garland, C., Pusede, S. E., Wooldridge, P. J., Ullmann, K., Hall, S. R., and Cohen, R. C.: Measurements of $\text{CH}_3\text{O}_2\text{NO}_2$ in the upper troposphere, *Atmos. Meas. Tech.*, 8, 987–997, doi:10.5194/amt-8-987-2015, 2015.
- Osthoff, H. D., Brown, S. S., Ryerson, T. B., Fortin, T. J., Lerner, B. M., Williams, E. J., Pettersson, A., Baynard, T., Dubé, W. P., Ciciora, S. J., and Ravishankara, A. R.: Measurement of atmospheric NO_2 by pulsed cavity ring-down spectroscopy, *J. Geophys. Res.*, 111, D12305, doi:10.1029/2005JD006942, 2006.
- Pandey, S. K., Kim, K. H., Chung, S. Y., Cho, S. J., Kim, M. Y., and Shon, Z. H.: Long-term study of NO_x behavior at urban roadside and background locations in Seoul, Korea, *Atmos. Environ.*, 42, 607–622, doi:10.1016/j.atmosenv.2007.10.015, 2008.
- Penkett, S., Gilge, S., Plass-Duelmer, C., Galbally, I., Brough, N., Bottenheim, J. W., Flocke, F. M., Gerwig, H., Lee, J. D., Milton, M., Roher, F., Ryerson, T. B., Steinbacher, M., Torseth, K., Wielgosz, R., Suda, K., Akimoto, H., and Tarasova, O.: A WMO/GAW Expert Workshop on Global Long-term Measurements of Nitrogen Oxides and Recommendations for GAW Nitrogen Oxides Network, Hohenpeissenberg, Germany, 8–9 October 2009, WMO TD No. 1570, 45 pp., February 2011.
- Peterson, C. and Honrath, R. E.: NO_x and NO_y over the northwestern North Atlantic: measurements and measurement accuracy, *J. Geophys. Res. Atmos.*, 104, 11695–11707, doi:10.1029/1998JD100088, 1999.
- Pollack, I. B., Lerner, B. M., and Ryerson, T. B.: Evaluation of ultraviolet light-emitting diodes for detection of atmospheric NO_2 by photolysis – chemiluminescence, *J. Atmos. Chem.*, 65, 111–125, doi:10.1007/s10874-011-9184-3, 2011.
- Ridley, B. A., Carroll, M. A., Torres, A. L., Condon, E. P., Sachse, G. W., Hill, G. F., and Gregory, G. L.: An intercomparison of results from ferrous sulphate and photolytic converter techniques for measurements of NO_x made during the NASA GTE/CITE 1 aircraft program, *J. Geophys. Res.*, 93, 15803–15811, doi:10.1029/JD093iD12p15803, 1988.
- Riemer, N., Vogel, H., Vogel, B., Schell, B., Ackermann, I., Kessler, C., and Hass, H.: Impact of the heterogeneous hydrolysis of N_2O_5 on chemistry and nitrate aerosol formation in the lower troposphere under photosmog conditions, *J. Geophys. Res.*, 108, 1–21, doi:10.1029/2002JD002436, 2003.
- 68 Roberts, J. M., Marchewka, M., Bertman, S. B., Sommariva, R., Warneke, C., de Gouw, J., Kuster, W., Goldan, P., Williams, E., Lerner, B. M., Murphy, P. and Fehsenfeld, F. C.: Measure-

- ments of PANs during the New England Air Quality Study 2002, *J. Geophys. Res.*, 112, D20306, doi:10.1029/2007JD008667, 2007.
- Roumelis, N. and Glavas, S.: Thermal decomposition of peroxyacetyl nitrate in the presence of O₂, NO₂ and NO, *Monatsh. Chem.*, 123, 63–72, doi:10.1007/BF01045298, 1992.
- Ryerson, T. B., Williams, E. J., and Fehsenfeld, F. C.: An efficient photolysis system for fast-response NO₂ measurements, *J. Geophys. Res.*, 105, 26447–26461, doi:10.1029/2000JD900389, 2000.
- Sadanaga, Y., Fukumori, Y., Kobashi, T., Nagata, M., Takenaka, N., and Bandow, H.: Development of a selective light-emitting diode photolytic NO₂ converter for continuously measuring NO₂ in the atmosphere, *Anal. Chem.*, 82, 9234–9239, doi:10.1021/ac101703z, 2010.
- Sander, S. P., Golden, D. M., Kurylo, M. J., Moorgat, G. K., Keller-Rudek, H., Wine, P. H., Ravishankara, A. R., Kolb, C. E., Molina, M. J., Finlayson-Pitts, B. J., Huie, R. E., and Orkin, V. L.: Chemical Kinetics and Photochemical Data for Use in Atmospheric Studies, Evaluation No. 17, JPL Publication 10-6, Jet Propulsion Laboratory, Pasadena, USA, available at: <http://jpldataeval.jpl.nasa.gov> (last access: 22 October 2015), 2011.
- Schott: Schott UG5 UV-passing filter, datasheet, available at: http://www.uggoptics.com/materials_filters_schott_uvTransmitting_UG5.aspx (last access: 25 July 2014), 1997.
- Sherwen, T., Evans, M. J., Carpenter, L. J., Andrews, S. J., Lidster, R. T., Dix, B., Koenig, T. K., Volkamer, R., Saiz-Lopez, A., Prados-Roman, C., Mahajan, A. S., and Ordóñez, C.: Iodine's impact on tropospheric oxidants: a global model study in GEOS-Chem, *Atmos. Chem. Phys.*, 16, 1161–1186, doi:10.5194/acp-16-1161-2016, 2016.
- Singh, H. W., Kanakidou, M., Crutzen, P. J., and Jacob, D. J.: High concentrations and photochemical fate of oxygenated hydrocarbons in the global troposphere, *Nature* 378, 50–54, doi:10.1038/378050a0, 1995.
- Skalska, K., Miller, J. S., and Ledakowicz, S.: Trends in NO_x abatement: a review., *Sci. Total Environ.*, 408, 3976–3989, doi:10.1016/j.scitotenv.2010.06.001, 2010.
- Stieb, D. M., Judek, S., and Burnett, R. T.: Meta-analysis of time-series studies of air pollution and mortality: effects of gases and particles and the influence of cause of death, age, and season, *J. Air Waste Manag. Assoc.*, 52, 470–484, doi:10.1080/10473289.2002.10470794, 2002.
- Talukdar, R. K., Burkholder, J. B., Hunter, M., Gilles, M. K., Roberts, J. M., and Ravishankara, A. R.: Atmospheric fate of several alkyl nitrates Part 2 UV absorption cross-sections and photodissociation quantum yields, *J. Chem. Soc. Faraday Trans.*, 93, 2797–2805, doi:10.1039/A701781B, 1997.

- Thornton, J. A., Wooldridge, P. J., and Cohen, R. C.: Atmospheric NO₂: in situ laser-induced fluorescence detection at parts per trillion mixing ratios, *Anal. Chem.*, 72, 528–39, 2000.
- Trebs, I., Mayol-Bracero, O. L., Pauliquevis, T., Kuhn, U., Sander, R., Ganzeveld, L., Meixner, F. X., Kesselmeier, J., Artaxo, P., and Andreae, M. O.: Impact of the Manaus urban plume on trace gas mixing ratios near the surface in the Amazon Basin: Implications for the NO-NO₂-O₃ photostationary state and peroxy radical levels, *J. Geophys. Res.*, 117, D05307, doi:10.1029/2011JD016386, 2012.
- Tuazon, E. C., Carter, W. P. L., and Atkinson, R.: Thermal decomposition of peroxyacetyl nitrate and reactions of acetyl peroxy radicals with NO and NO₂ over the temperature range 283–313 K, *J. Phys. Chem.*, 95, 2434–2437, doi:10.1021/j100159a059, 1991.
- Tuzson, B., Zeyer, K., Steinbacher, M., McManus, J. B., Nelson, D. D., Zahniser, M. S., and Emmenegger, L.: Selective measurements of NO, NO₂ and NO_y in the free troposphere using quantum cascade laser spectroscopy, *Atmos. Meas. Tech.*, 6, 927–936, doi:10.5194/amt-6-927-2013, 2013.
- Val Martin, M., Honrath, R. E., Owen, R. C., and Li, Q. B.: Seasonal variation of nitrogen oxides in the central North Atlantic lower free troposphere, *J. Geophys. Res.*, 113, D17307, doi:10.1029/2007JD009688, 2008.
- Villena, G., Bejan, I., Kurtenbach, R., Wiesen, P., and Kleffmann, J.: Interferences of commercial NO₂ instruments in the urban atmosphere and in a smog chamber, *Atmos. Meas. Tech.*, 5, 149–159, doi:10.5194/amt-5-149-2012, 2012.
- Volz-Thomas, A., Pätz, H.-W., Houben, N., Konrad, S., Mihelcic, D., Klüpfel, T., and Perner, D.: Inorganic trace gases and peroxy radicals during BERLIOZ at Pabstthum: An investigation of the photostationary state of NO_x and O₃, *J. Geophys. Res.*, 108, 8248, doi:10.1029/2001JD001255, 2003.
- Wang, W.-C., Liang, X.-Z., Dudek, M. P., Pollard, D., and Thompson, S. L.: Atmospheric ozone as a climate gas, *Atmos. Res.*, 37, 247–256, doi:10.1016/0169-8095(94)00080-W, 1995.
- Warneck, P. and Zerbach, T.: Synthesis of peroxyacetyl nitrate in air by acetone photolysis, *Environ. Sci. Technol.*, 26, 74–79, doi:10.1021/es00025a005, 1992.
- Whalley, L. K., Lewis, A. C., McQuaid, J. B., Purvis, R. M., Lee, J. D., Stemmler, K., Zellweger, C., and Ridgeon, P.: Two high-speed, portable GC systems designed for the measurement of non-methane hydrocarbons and PAN: results from the Jungfraujoch High Altitude Observatory, *J. Environ. Monit.*, 6, 234–41, doi:10.1039/b310022g, 2004.

- Williams, J. E., Le Bras, G., Kukui, A., Ziereis, H., and Brenninkmeijer, C. A. M.: The impact of the chemical production of methyl nitrate from the $\text{NO} + \text{CH}_3\text{O}_2$ reaction on the global distributions of alkyl nitrates, nitrogen oxides and tropospheric ozone: a global modelling study, *Atmos. Chem. Phys.*, 14, 2363-2382, doi:10.5194/acp-14-2363-2014, 2014.
- Winer, A. M., Peters, J. W., Smith, J. P., and Pitts, J. N.: Response of Commercial Chemiluminescent NO-NO₂ Analyzers to Other Nitrogen-Containing Compounds, *Environ. Sci. Technol.*, 8, 1118–1121, doi:10.1021/es60098a004, 1974.
- Yang, J., Honrath, R. E., Peterson, M. C., Parrish, D. D., and Warshawsky, M.: Photostationary state deviation—estimated peroxy radicals and their implications for HO_x and ozone photochemistry at a remote northern Atlantic coastal site, *J. Geophys. Res.*, 109, D02312, doi:10.1029/2003JD003983, 2004
- Zabielski M. F., Seery, D. J., Dodge, L. G.: Influence of mass transport and quenching on nitric oxide chemiluminescent analysis, *Environ. Sci. Technol.*, 18, 88–92, doi:10.1021/es00120a007, 1984.
- Zhang, L., Wiebe, A., Vet, R., Mihele, C., O'Brien, J. M., Iqbal, S., and Liang, Z.: Measurements of reactive oxidized nitrogen at eight Canadian rural sites, *Atmos. Environ.*, 42, 8065–8078, doi:10.1016/j.atmosenv.2008.06.034, 2008.

Table 1. Comparison of the NO_2 observed from measurement of three zero air sources. (Eco Physics AG PAG 003, BOC Specialty Gasses BTCA 178, and Sofnofil/Carbon/ $13\times$ molecular sieve filters) by LIF. The average of ten 1 min averages is shown in pptv, normalized to the lowest reading, in raw PMT counts s^{-1} as well as the standard deviation of those averages.

	PAG 003	BTCA 178	Sofnofil/Carbon
Normalized concentration (pptv)	23.06	26.17	-
Signal (counts s^{-1})	88.10	88.66	83.95
Standard Deviation	1.64	1.56	1.81

Table 2. Effect of varying the residence time of PAN (1.0 ppb) within a 2.7 m PFA inlet on measured NO₂ concentrations.

	Inlet residence time (s ⁻¹)			
	0.84	1.05	1.40	2.10
NO ₂ (ppt)	60.2	61.3	60.6	61.5
NO ₂ (%)	5.4	5.4	5.2	5.3

Table 3. Peak surface temperature and current drawn by BLC lamps in a bench test at 20.0 °C showing converter efficiency, current, and surface temperature.

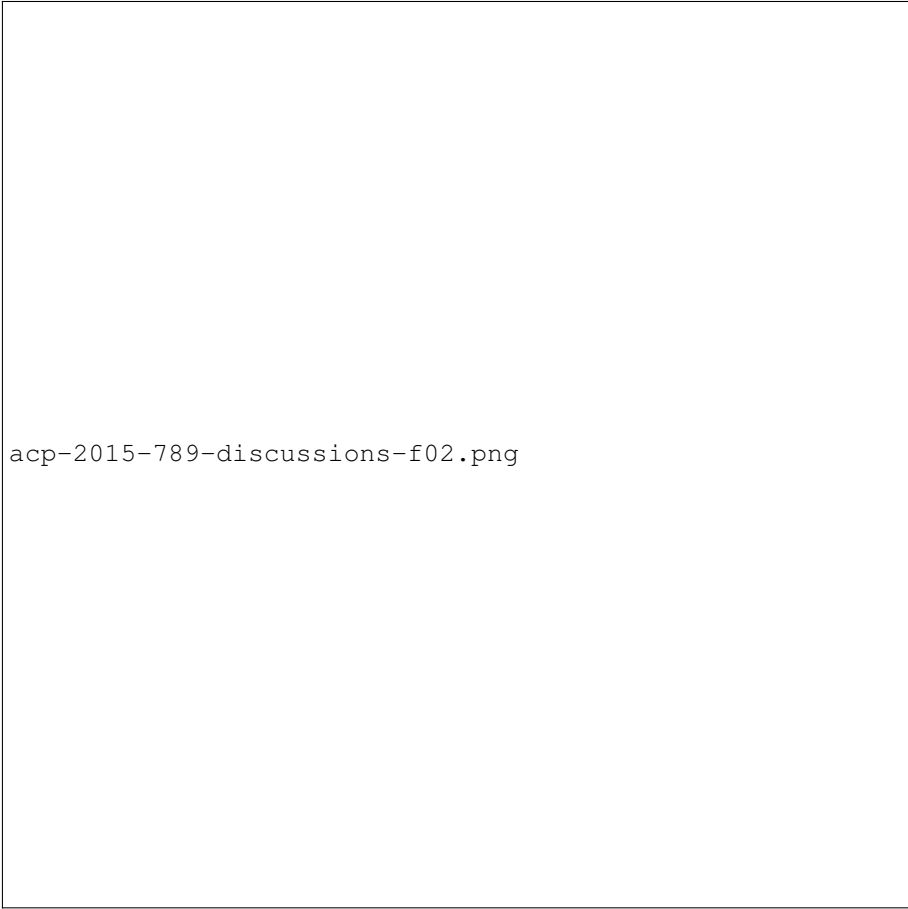
Lamp No.	Converter efficiency (%) ± 1	BLC Lamp Surface Temperature ($^{\circ}\text{C}$) ± 0.05	Current Draw (A) ± 0.0005
1	41	79.8	0.969
2		75.3	0.953
3	35	77.6	0.933
4		74.0	0.931
5	22	76.2	0.916
6		56.4	0.567

Table 4. The average percentage conversion of PAN to NO₂ measured, and normalized to the converter efficiency of each BLC.

	Converter efficiency (%) ± 1		
	41	35	22
Measured %	10.8	15.9	19.6
Normalized %	4.4	5.2	4.3

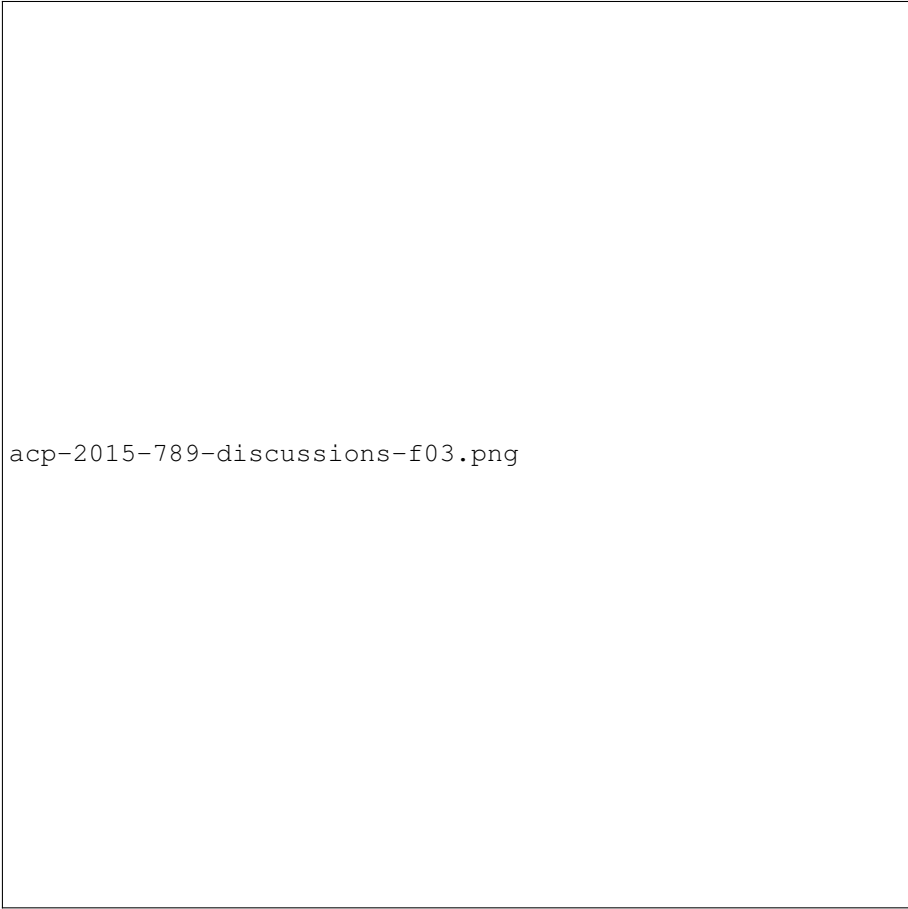


Figure 1. The average raw counts s^{-1} (left) and pptv (right) recorded by a LIF instrument when sampling various mixing ratios of PAN (in red) and zero air (black). The variance of the zero air signal is also shown (dashed black). The average signal while sampling PAN falls within the noise of the zero signal.



acp-2015-789-discussions-f02.png

Figure 2. The measured NO_2 artifact signal (left panel) of the supplied PAN mixing ratio, and as a percentage (right panel), for three BLC units operating in constant mode separated by NO_2 conversion efficiency: Green = 41 %, Red = 35 %, Blue = 22 %.



acp-2015-789-discussions-f03.png

Figure 3. The measured NO_2 artifact signal as a function of the supplied PAN mixing ratio (left panel), and as a percentage (right panel), for three BLC units operating in switching mode separated by NO_2 conversion efficiency: Green = 41 %, Red = 35 %, Blue = 22 %.

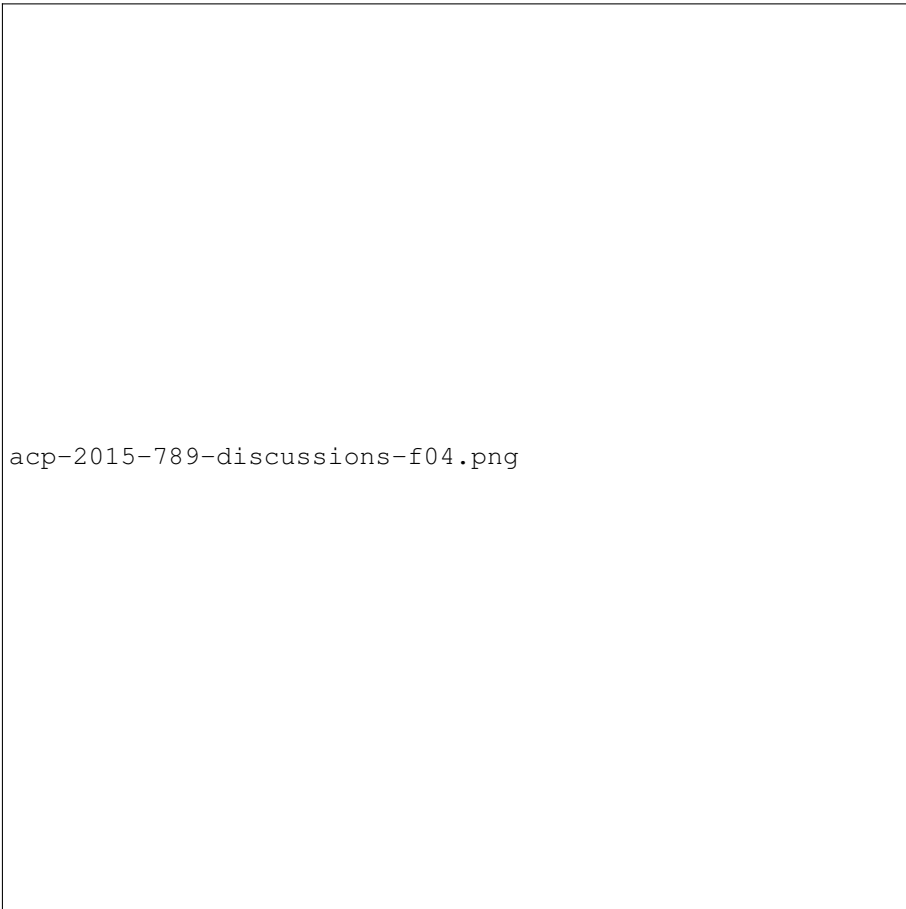
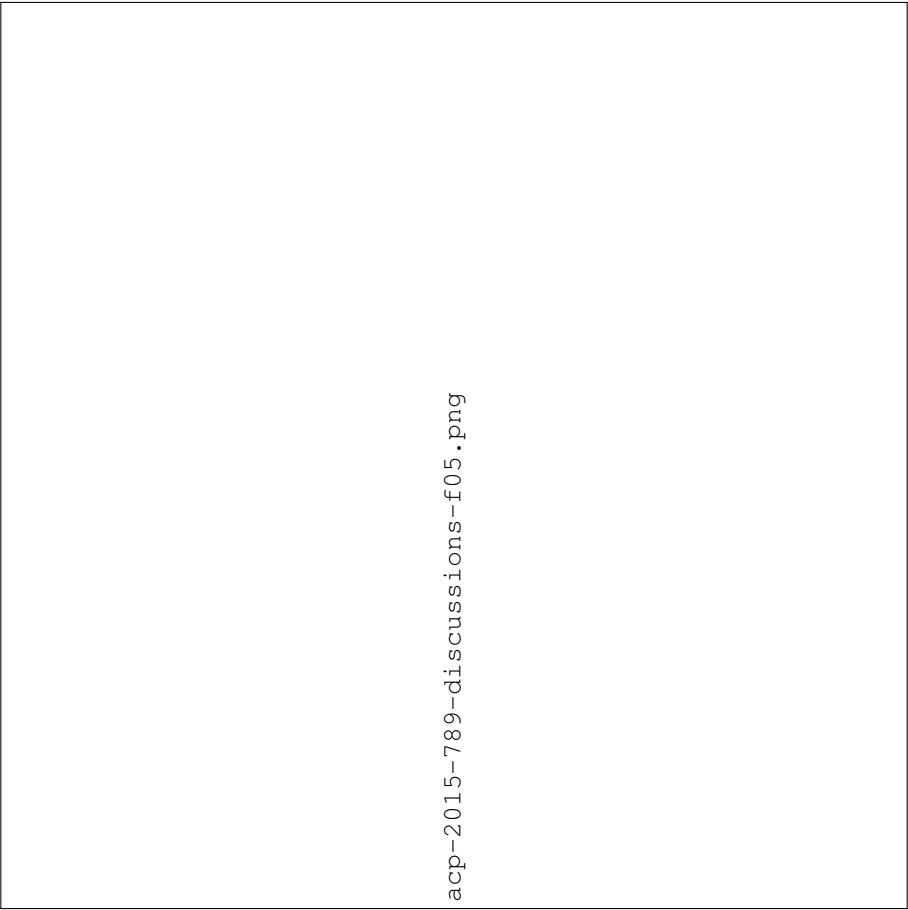


Figure 4. The measured NO_2 artifact signal as a function of the supplied PAN mixing ratio (left panel), and as a percentage (right panel), for the cooled (blue) and uncooled (red) high powered BLC.



acp-2015-789-discussions-f05.png

Figure 5. Shown is the spectral output vs. wavelength of two new, previously unused BLC lamps No. 1 (solid) and 2 (dashed) in green, two used lamps No. 3 (solid) and 4 (dashed) in red; still within acceptable conversion efficiency, and two which fall below acceptable limits No. 5 (solid) and 6 (dashed) in blue. The NO_2 quantum yield is shown in black.

acp-2015-789-discussions-f06.png

Figure 6. Absorption cross section (red) and quantum yield (dashed black) of NO_2 , presented with the spectral output of UG5 optical filtering (purple) and an average of the six BLC lamps used in this study output (dark blue). Shown are interfering species; NO_3 radicals (green), HONO (light blue), BrONO_2 (lilac) which are overlapped significantly by the UG5 optics – completely in the case of HONO, whilst much less overlap is exhibited by the UV-LEDs of the BLC. Also shown is PAN (gold), which clearly is not overlapped by either UG5 or BLC light sources. Additional non-interfering species; ClONO_2 (triangles), N_2O_5 (squares), HO_2NO_2 (circles), HNO_3 (diamonds) shown for reference.

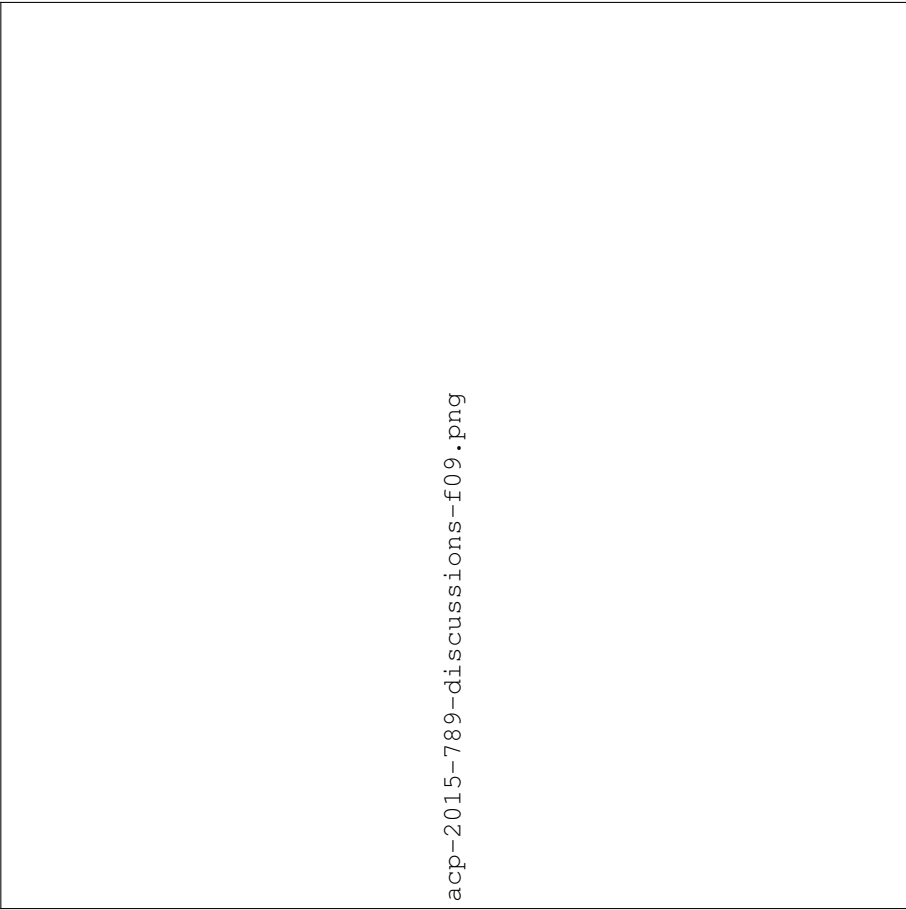


acp-2015-789-discussions-f07.png

Figure 7. Model of thermal decomposition of PAN to NO_2 with a residence time of 0.96 s at temperatures between 0 to 150 °C. Inset is detail of 45 to 85 °C. The red shaded area corresponding to the temperature range of the UV LEDs of a BLC. Kinetic data from IUPAC (Atkinson et al., 2006)

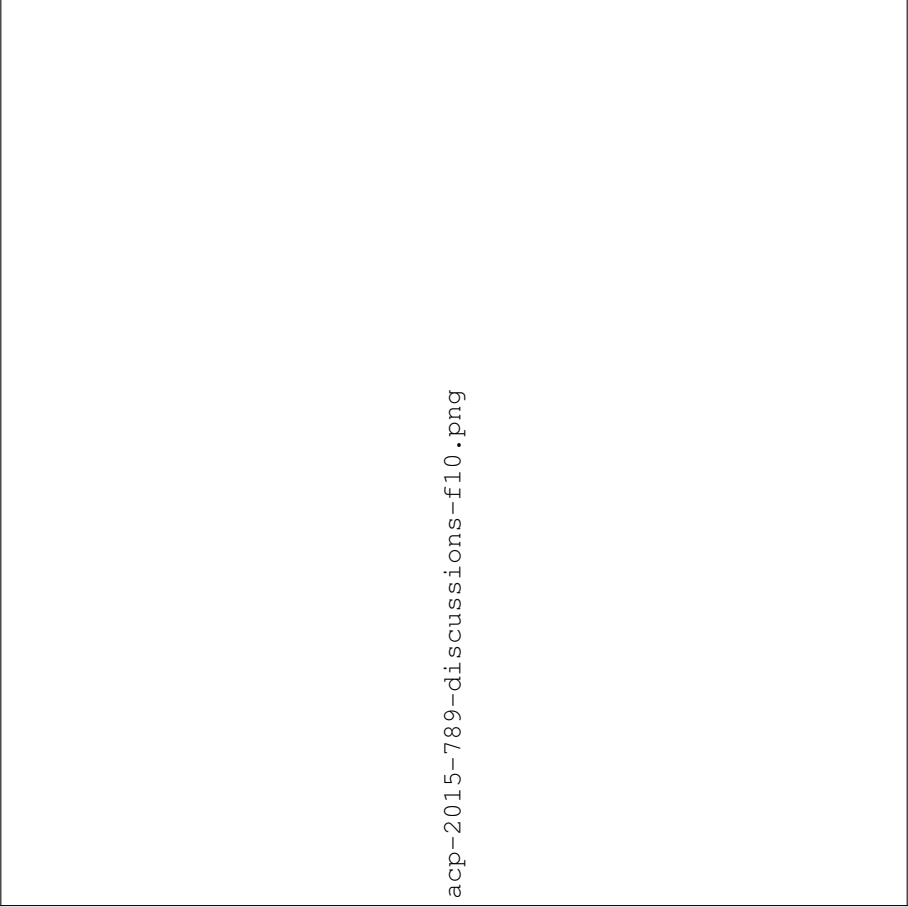
acp-2015-789-discussions-f08.png

Figure 8. Thermal decomposition profiles of IONO_2 \blacklozenge ; BrONO_2 \circ ; ClONO_2 \blacktriangleright ; HO_2NO_2 \bullet ; N_2O_5 \blacktriangleleft ; $\text{C}_2\text{H}_5\text{O}_2\text{NO}_2$ \diamond ; $\text{CH}_3\text{C}(\text{O})\text{CH}_2\text{O}_2\text{NO}_2$ \square ; MPAN \blacksquare ; PAN \blacktriangle ; PPN \blacktriangledown . Calculated from IUPAC recommended kinetic data (Atkinson et al, 2004, 2006, 2007) using FACSIMILE kinetic modelling software (MCPA Software Ltd.) based on 1 s residence time. Note $\text{CH}_3\text{O}_2\text{NO}_2$ is not shown but has the same profile as $\text{CH}_3\text{C}(\text{O})\text{CH}_2\text{O}_2\text{NO}_2$.



acp-2015-789-discussions-f09.png

Figure 9. GEOS-Chem model output showing the monthly maximum percentage over-reporting of NO₂ determined by BLC/Chemiluminescence **(a)** zonally and **(b)** by altitude in any month of a 1 year simulation. Panels **(c)** and **(d)** show the same in absolute pptv values. Surface values are the maximum over-reporting in any month, zonal values are the maximum over reporting in any month and in any of the longitudinal grid boxes. The MD160 cruise track of Hosaynali-Beygi et al., (2011) is also shown in panels **(a)** and **(c)** as are the locations of the studies of; Bauguitte et al. (2012) ★; Frey et al. (2013, 2015) ▲; Griffin et al., (2007) ●; Kanaya et al., (2007) ■; Yang et al., (2004) ◆.



acp-2015-789-discussions-f10.png

Figure 10. Leighton ratio calculated for each surface model grid-box for each daylight hour for March by the GEOS-Chem model as a function of the grid box NO_2 concentration. The instrument interference is characterized by a numerical solution of Eq. (5) with $\tau = 0.42\text{ s}$ and a residence time of 1 s. Red shows the values calculated without the interference on the NO_2 concentration and the blue indicated the values calculated with the interference. The interferences are calculated for different lamp temperatures, 20 to 95 °C.